RI 9128

Bureau of Mines Report of Investigations/1987

Physical Properties and Mechanical Cutting Characteristics of Cobalt-Rich Manganese Crusts

By D. A. Larson, S. Tandanand, M. L. Boucher, M. S. Olson, R. J. Morrell, and R. E. Thill

UNITED STATES DEPARTMENT OF THE INTERIOR

Report of Investigations 9128

Physical Properties and Mechanical Cutting Characteristics of Cobalt-Rich Manganese Crusts

By D. A. Larson, S. Tandanand, M. L. Boucher, M. S. Olson,
R. J. Morrell, and R. E. Thill

UNITED STATES DEPARTMENT OF THE INTERIOR
Donald Paul Hodel, Secretary

BUREAU OF MINES
David S. Brown, Acting Director

Library of Congress Cataloging in Publication Data:

Physical properties and mechanical cutting characteristics of cobalt-rich manganese crusts.

(Report of investigations/ Bureau of Mines ; 9128)

Bibliography: p. 22

Supt. of Docs. no.: I 28.23: 9128.

1. Manganese nodules. I. Larson, David A. II. Series: Report of investigations (United States. Bureau of Mines) ; 9128.

TN23.U43 [TN538.M35] 622 s [553.4'629] 87-600147

CONTENTS

ILLUSTRATIONS

ILLUSTRATIONS--Continued

TABLES

UNIT OF MEASURE ABBREVIATIONS USED IN THIS REPORT

cm	centimeter	kN	kilonewton
cm/min	centimeter per minute	kV	kilovolt
°C	degree Celsius	m	meter
g/cm^3	gram per cubic centimeter	µm	micrometer
GPa	gigapascal	mm	millimeter
h	hour	MPa	megapascal
in	inch	N	newton
in/min	inch per minute	nA	nanoampere
J	joule	pct	percent
J/cm^3	joule per cubic centimeter	yr	year
km/s	kilometer per second		

PHYSICAL PROPERTIES AND MECHANICAL CUTTING CHARACTERISTICS OF COBALT-RICH MANGANESE CRUSTS

By D. A. Larson,[1] S. Tandanand,[1] M. L. Boucher,[2] M. S. Olson,[3] R. J. Morrell,[4] and R. E. Thill[5]

ABSTRACT

The Bureau of Mines conducted research to develop preliminary engineering data necessary if the cobalt-rich manganese crusts that occur in the Exclusive Economic Zone (EEZ) of the Hawaiian Archipelago are to be mined. The research was divided into the following sections: (1) physical, mineralogical, and chemical descriptions; (2) mechanical property testing, such as compressive strength, tensile strength, and a rippability index; and (3) mechanical cutting characteristics, including average and peak cutter forces, the specific energy, and cuttings size distribution. Section 1 utilized microscope, X-ray powder diffractometer, and electron microprobe analyses. Section 2 utilized standard mechanical property testing techniques. Section 3 utilized a converted planer mill with full-size coal cutters to fragment the crust and substrate samples.

The manganese crust samples were mainly manganese and iron oxides and hydroxides with an average cobalt content of 1 pct and had a nucleus or substrate of rock or sediment. The significant results shown by the mechanical property and cutting tests are that the crust and all but two types of substrates (basalt and trachyte) are weak materials and easily cut with standard drag cutters. The crusts are generally comparable to medium hard coal in strength and in their resistance to cutting.

[1]Mining engineer.
[2]Geologist.
[3]Engineering technician.
[4]Supervisory mining engineer.
[5]Supervisory geophysicist.
Twin Cities Research Center, Bureau of Mines, Minneapolis, MN.

INTRODUCTION

The purpose of the Bureau's research was to begin development of a detailed engineering data base for the cobalt-rich manganese crusts that occur in the Exclusive Economic Zone (EEZ) of the United States. This report covers test results of the physical and mechanical properties that would be required for mine planning. Chemical and petrographic analyses are included as a part of the sample descriptions. Each of the three sections contains a complete description of the equipment and procedures used.

The cobalt-rich manganese crusts investigated in this study were collected from seamounts in the Hawaiian Archipelago. According to Cruickshank (1),[6] the crusts of interest for mining occur primarily at depths between 800 and 2,400 m on seamounts and submerged slopes of islands. The crusts form on exposed rock surfaces, including basalt, hyaloclastite, and/or phosphorite. Average crust thickness over areas of sufficient size to be commercially attractive may be no more than 2 cm (2). Crust samples from the Hawaiian Archipelago and Johnston Islands may average as much as 1.0 pct Co (1), three to four times richer than nodules (2), and may form a valuable source of this strategic element.

Johnson (3) has grouped the manganese deposits into six types. The type most suitable for mining are the type F (crust payments). The major features of the crust pavement, as defined by Johnson, have been summarized by Latimer (2) as follows:

1. May be common in the Johnston Island and Necker Ridge areas.
2. Pavement may cover tens of square kilometers.
3. Pavement has a microrelief of a few centimeters with an average relief of less than 5 cm, although surface may be highly botryoidal.
4. Maximum slope of crust pavement areas is 16° to 20°.
5. Substrate material may be basalt or hyaloclastite.

Potential mining of these cobalt-rich manganese crusts has been discussed by Cruickshank (1) and Latimer (2). They stressed the need for more complete and accurate data engineering properties, both in the laboratory and in situ, before the development of suitable mining systems can begin. The information contained in this report provides some of these much needed data.

The first section of the report describes physical, mineralogical, and chemical characteristics of the samples tested. The descriptions includes both the crust and the substrates upon which the crust formed. Mineralogical analyses were performed using both optical and X-ray diffraction techniques. The chemical or elemental analyses of selected crust samples were performed with an electron microprobe and included determination of the cobalt, manganese, silicon, nickel, and iron contents.

The second section of this report provides data on the mechanical properties of the crust samples. It builds upon previous work by the Bureau, by testing a larger number and variety of crust and substrate samples. In addition, the current work was performed on samples that had been immersed in seawater from the time of collection to the end of testing. The properties measured include compressive strength, tensile strength, cohesive strength, angle of internal friction, shore hardness, and density.

The last section of the report provides data on the mechanical cutting characteristics of both crust and substrate materials. All testing was performed with a drag cutter because of the softness of the crust material. Other types of cutters, such as percussive or roller, may be equally suited, but this would need to be verified by additional testing. The data provided by the drag cutter tests include the average and peak forces acting on the bit, the specific energy of the cutting process, and the size distribution of the cuttings.

[6]Underlined numbers in parentheses refer to items in the list of references preceding the appendixes.

A final note of caution is advised before the results of this research program are put into use. Because of the length of time in storage (approximately 1 yr), some deterioration of the samples may have occurred, thereby affecting test results. In addition, the limited number of available samples minimized the number of tests that could be performed; thus the results may need to be modified as more test data become available. However, this report provides the most comprehensive engineering analysis available of the cobalt-rich manganese crusts.

DESCRIPTION OF CRUST SAMPLES

LOCATION AND IDENTIFICATION

A total of 18 samples of cobalt-rich manganese crust were tested. The samples were generally tabular in shape and had crust coatings that ranged in thickness from 0.1 to 3.2 cm. The samples were collected from areas along the north and south side of the Hawaiian Archipelago at water depths between 500 to 4,400 m. All samples were kept immersed in seawater to prevent air drying deterioration and most samples had been in storage for at least 1 yr before testing. Upon receipt at the Twin Cities Research Center, all samples (A through Y) were cataloged and photographed. As the research progressed, some samples were dropped from the test program because they were too friable for sample preparation or would yield very limited engineering data. The letter identification and general location and description of the samples is given in table 1. Photographs of representative crust samples tested are shown in figures 1 and 2.

TABLE 1. - Sample site location, description, and characterization methods

Sample[1]	Size, cm	Crust thickness, cm	Location	Depth, m	Type of test performed[2]
			BASALTIC		
B.....	10 by 20 by 25	1.9	25°16.58' N, 162°04.05' W	2,300-3,000	PP, CT, PT
C.....	6 by 13 by 15	3.2	25°58.80' N, 164°22.75' W	1,300-1,800	CT, PT
D.....	7 by 11 by 11	1.3	29°38.03' N, 179°17.35' E	1,600-1,900	CT, CH, PT
F.....	10 by 15 by 17	1.6	23°40.33' N, 164°53.43' W	1,000-1,650	CT, PT
G.....	13 by 22 by 23	1.6	25°16.58' N, 162°04.05' W	2,300-3,000	PP, CT, CH, PT
H.....	6 by 13 by 15	2.5	23°57.35' N, 164°24.87' W	950-1,300	CT, PT
I.....	8 by 11 by 18	2.2	23°57.35' N, 164°24.87' W	950-1,300	CT, PT
J.....	10 by 14 by 15	3.0	19°28.87' N, 157°03.24' W	2,500-2,750	PP, CT, PT
K.....	9 by 11 by 23	2.5	29°09.77' N, 174°04.26' W	800- 920	PT
L.....	4 by 17 by 20	2.2	23°59.26' N, 164°21.80' W	1,900-2,100	PT
M.....	10 by 15 by 20	1.3	28°44.35' N, 178°47.08' W	2,700-3,000	PP, CT, CH, PT
N.....	5 by 13 by 20	2.5	25°58.80' N, 164°22.75' W	1,300-1,800	CT, PT
			TRACHYTIC[3]		
O.....	10 by 13 by 20	1.5	18°37' N, 158°18' W	500-4,400	PP, CH, PT
S.....	5 by 23 by 23	1.6	18°37' N, 158°18' W	500-4,400	PT
T.....	10 by 18 by 18	1.9	18°37' N, 158°18' W	500-4,400	PT
U.....	9 by 15 by 20	.2	18°37' N, 158°18' W	500-4,400	PP, PT
X.....	10 by 15 by 25	2.2	18°37' N, 158°18' W	500-4,400	PT
Y.....	15 by 20 by 33	3.8	18°37' N, 158°18' W	500-4,400	PP, CT, CH, PT

[1]See appendix A for a complete description of samples.
[2]CH, chemical; CT, cutting test; PP, physical property; PT, petrographic.
[3]Samples collected from the Cross Seamount.

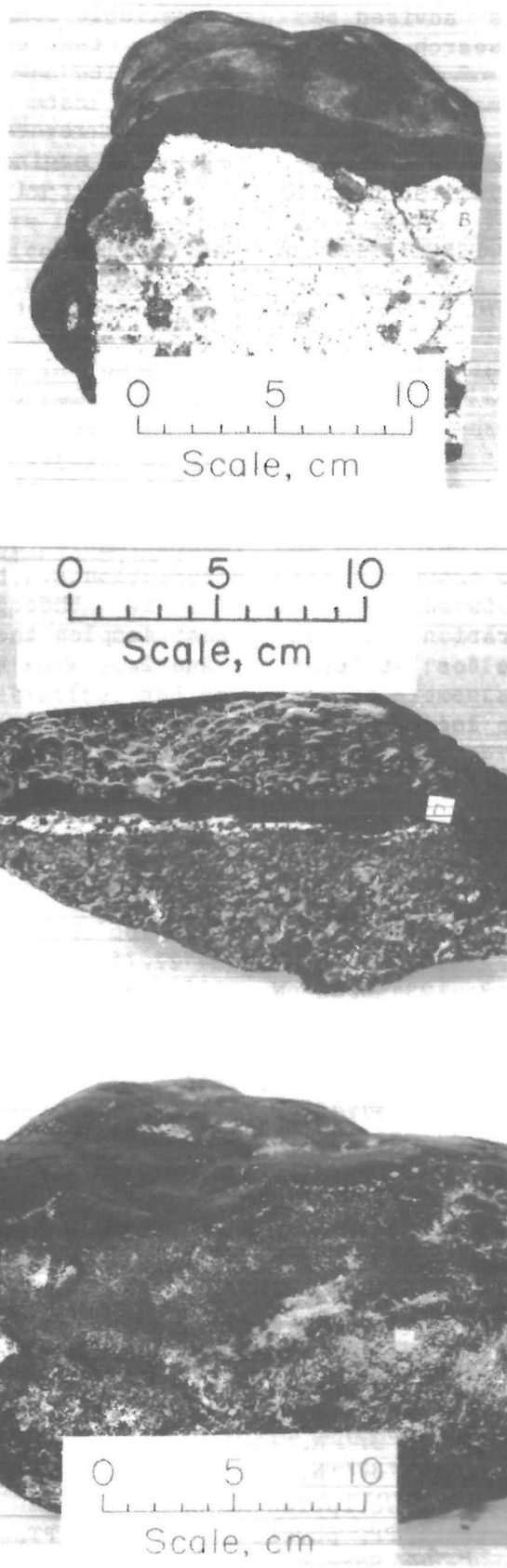

FIGURE 1.—Representative crust samples. Sample B, showing altered basalt substrate (top), sample D (middle), and sample G (bottom).

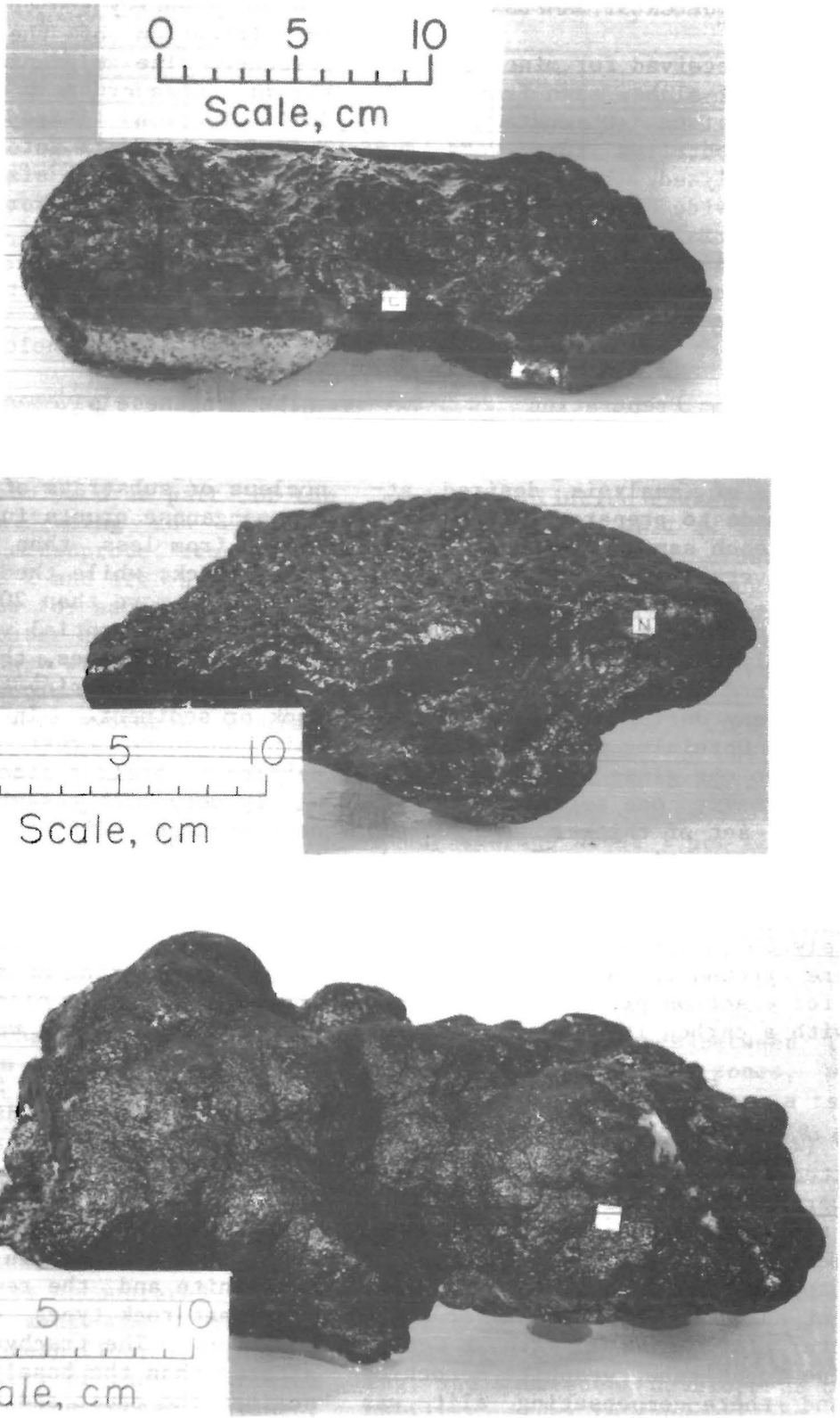

FIGURE 2.—Representative crust samples. Sample L (top), sample N and basalt substrate (middle), and sample Y (bottom).

ANALYSIS OF CRUST SAMPLES

The samples received for mineral analysis consisted of slabs, sawn from larger pieces of crust and substrate. These were the only portions that were described and analyzed, but every effort was made to provide samples representative of the materials used for the property tests in this study. All samples are referred to consistently in the text, tables, and appendixes by the letter designation.

Specimen Preparation

Because of the small amount of material and the types of analysis desired, attempts were made to prepare polished thin sections for each sample. The wet samples became very fragile on drying and would crumble. To prepare sections, the samples were partially dried and impregnated with polyester resin; then resawed, ground flat, and impregnated several more times with epoxy during the thin sectioning process. Obtaining proper bonding of the samples to the glass slide was difficult, but finally one set of thin sections and a set of thicker (50-100 μm) polished thin sections were produced. The crusts to be X-rayed were thoroughly dried during initial preparation at approximately 50° C in a vacuum oven, and then were ground in an agate mortar. Samples for electron probe analysis were coated with a carbon in a vacuum coater.

Equipment

Zeiss[7] (WL pol Ultaphot II) polarizing transmitted and reflected light microscopes were used for the optical analysis and for the photomicrographs. A Polaroid MP-3 camera was used to take the remaining photographs. A Philips Electronic Instrument automated X-ray powder diffractometer (APD 3600/01) with a Copper long, fine focus tube, graphite monochromator and theta-compensating slit was used to identify and confirm the optical identification of the mineral phases present. The elemental composition of the manganese crusts was analyzed using a JEOL electron microprobe (733) with Tractor-Northern automation (TN-5500, 5600), a 1-μm spot size at 20 kV and 20 nA, and the Tracor-Northern ZAF correction program.

[7]Reference to specific products does not imply endorsement by the Bureau of Mines.

Results

Morphology

The manganese pavement or crust deposits are comprised mainly of manganese and iron oxides and hydroxides and have a nucleus or substrate of rock or sediment. The manganese crusts in the present suite range from less than 1 mm to more than 30 mm thick; while the substrate nucleus is usually more than 20 mm thick and represents a substantial volume of waste.

In some instances, the crust occurs as a thin layer covering extensive areas of rock or sediment. In other instances, a thin manganese crust completely covers pebble- to boulder-size pieces, and outwardly very much resembles actual manganese nodules. Difference in thickness of the crust on opposite sides of cobbles are seen (one side thicker than the other and rapidly thinning at the middle) similar to the type of occurrences in nodules (4). The breaking up and recementing, by crusts, of both older manganese crust and rock fragments was also noted in these samples.

These samples are from a number of localities and major differences might be expected. However, the morphology and chemistry of the manganese crusts are very similar and only two very different subtrates were found. Samples from the Cross Seamount are an unusual trachytic sanidinite and the rest of the samples represent rock types of a basaltic composition. The trachytes are much less altered than the basalts. Appendix A describes the crust and subtrates generally and presents descriptions of the individual samples including photographs of cross sections of representative samples.

TABLE 2. - Microprobe analyses of five manganese crusts,[1] weight percent

Sample	Co		Fe		Mn		Ni		Si	
	Av	Range	Av	Range	Av	Range	Av	Range	Av	Range
G.....	1.5	1.2-2.2	12.6	10.1-14.7	29.7	22.5-35.6	0.7	0.3-1.1	1.4	1.0-1.8
D.....	.8	.5-1.4	15.9	12.5-17.8	22.0	18.6-24.0	.4	.2-0.6	2.5	1.4-3.4
M.....	.9	.5-1.4	15.6	13.8-18.4	24.5	18.1-32.0	.4	.2-0.7	2.1	1.5-3.0
O.....	.9	.4-1.2	14.1	11.1-21.1	23.5	15.6-28.4	.5	.1-0.8	2.0	1.1-4.4
Y.....	1.1	.9-1.1	11.5	9.4-14.0	30.0	25.2-34.5	.8	.6-1.1	1.1	.9-1.6

[1]10 different points on each crust.

NOTE.---Estimated error due to X-ray statistics: Mn and Fe, ±1.0; Co, Si, and Ni, ±0.2.

Chemistry

The metal content of the manganese crusts was also analyzed as part of the sample description, using the electron microprobe. The microprobe results are presented in table 2 and are averages of 10 different points for each sample, selected from the outer edge of the crust to the inner boundary with the substrate. Areas close to fractures and rough, poorly polished zones were avoided. Accurate wavelength dispersive microprobe analysis requires a fairly smooth surface. As the analyses show, the crust compositions are very heterogeneous. The range given in table 2 shows the lowest and highest analysis of the 10 spots for each crust sample. These are single analyses, with no replications, so no error is given other than that estimated to be due to X-ray counting statistics.

Analysis showed that most zones contain more manganese than iron. (In a few samples analyzed, not reported here, the manganese and iron were about equal or iron was greater.) The 1-μm spot analyses show the typical elemental values for manganese, iron, cobalt, silicon, and nickel that occur in the crust. During actual mining of the pavements, some unavoidable dilution caused by the recovery of substrate, as well as the goethite and clay fraction in the crust, will lower the metal content of manganese, cobalt, and nickel. Therefore, any bulk analyses of the crusts with attached substrate will be lower than those reported here. Without a ratio of crust to substrate that would vary widely with mining methods and area mined, no estimates can be given of ore grades or bulk analyses.

Almost all the crusts analyzed in this study average about 1 pct cobalt with at least 0.4 pct as the lowest value found. The higher cobalt content correlates with a higher manganese and lower iron content of the individual layer. There are no indications of a specific cobalt mineral that could be beneficiated. However, there are differences between the high-iron and high-manganese zones, which can be seen microscopically as a tarnishing of the high-iron, low-manganese, and low-cobalt zones.

MECHANICAL PROPERTY TESTING

A critical problem encountered in the mine planning for manganese crust recovery from the ocean floor is the extraction and delivery of the crust from the seal floor to the ocean surface. Thus, for equipment design purposes it is essential at the outset that mechanical properties of the crust and substrates be obtained. Dredged samples comprising manganese crust, hyaloclastite (altered basalt), and phosphoritic[8] material in the EEZ of Hawaiian Archipelago were obtained for conducting preliminary testing, and subsequent development of a rippability index to suggest how easily mechanical machines might mine manganese crusts.

[8]This section includes the trachytes with the phosphorites.

The first batch of dredged samples received contained unknown amounts of moisture. These samples were oven dried in a vacuum oven at 105° C for a minimum of 24 h to a standardized dry condition before testing. The results of the Bureau's preliminary tests on these dry materials were included in a presentation at the 1986 Offshore Technology Conference in Houston, TX, by Cruickshank (1).

A limited quantity of additional seabed samples were subsequently received. These samples were preserved in the original seawater. Mechanical and physical property tests were also conducted on these samples. The results are given in this report for comparison with the values obtained for the dry condition (1).

SAMPLE PREPARATION

Dimensions of the test samples for mechanical property determination were restricted by the thickness, size, and shape of the collected samples. For this reason, the test samples normally could not conform to recommended test standards (fig. 3). The manganese crust was weak and so thin that the cylinder size preferred for testing (2-in diam by 4-in length) was impossible to obtain. Moreover, the crustal samples were too friable to core drill. Hence, the irregular crustal samples were cut into small rectangular prisms; first by using a bandsaw, and next by trimming the edges of the prism to form a polyhedron (fig. 4). Both ends of the sample were cut and smoothed using a belt sander. With the aid of a spring loading device to provide a good grip in a lathe with a tool post grinder, the polyhedron sample was machined to a cylindrical shape (fig. 5).

Finally, the sample ends were machined using a surface grinder to maintain end parallelism (fig. 5). At this stage, the sample was ready for a sequence of both nondestructive and destructive tests. Whenever cylindrical samples could not be obtained by the method described because of the friability of the samples, rectangular prismatic samples were prepared, using the same procdure to ensure sample-end smoothness and parallelism. For saturated testing, prepared samples were presoaked in a brine having density of 1.02 g/cm^3.

TEST RESULTS

Mechanical Properties

The procedures for determining the mechanical properties, except for cohesive strength and angle of internal friction, were described earlier (5). The mechanical properties obtained from the oven-dried samples are compared in table 3 with properties of coal and Icelandic hyaloclastites. Because cohesive strength and angle of internal friction could not be obtained by standard procedures owing to constraints in sample preparation, these two properties were determined graphically by drawing a tangent between two Mohr's circles representing the state of stress at failure by the indirect tensile strength (Brazilian)

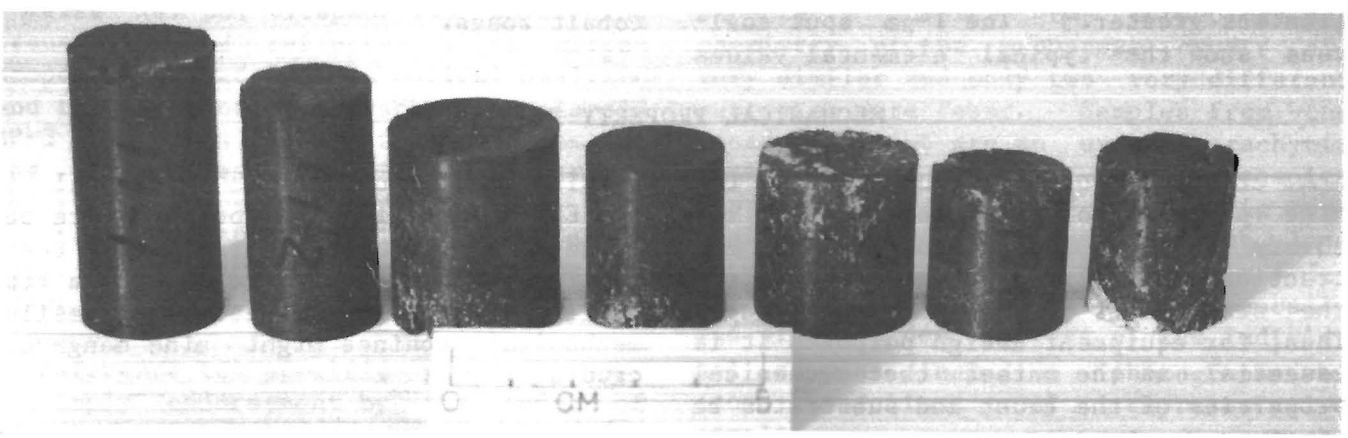

FIGURE 3.—Manganese crust prepared test samples. Note irregularities in the test samples.

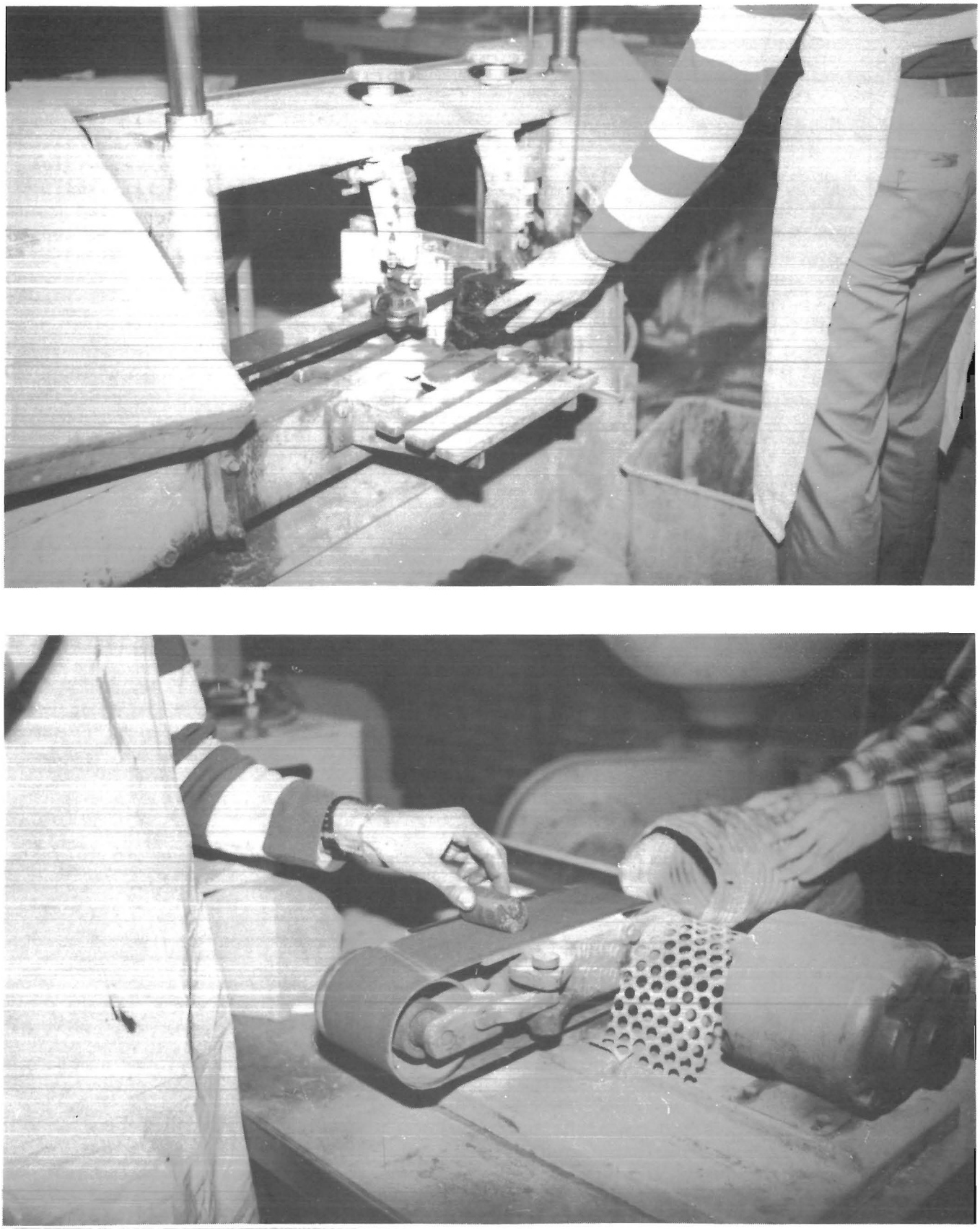

FIGURE 4.—Test sample being cut with bandsaw (top) and preparation of cylindrical sample using belt sander (bottom).

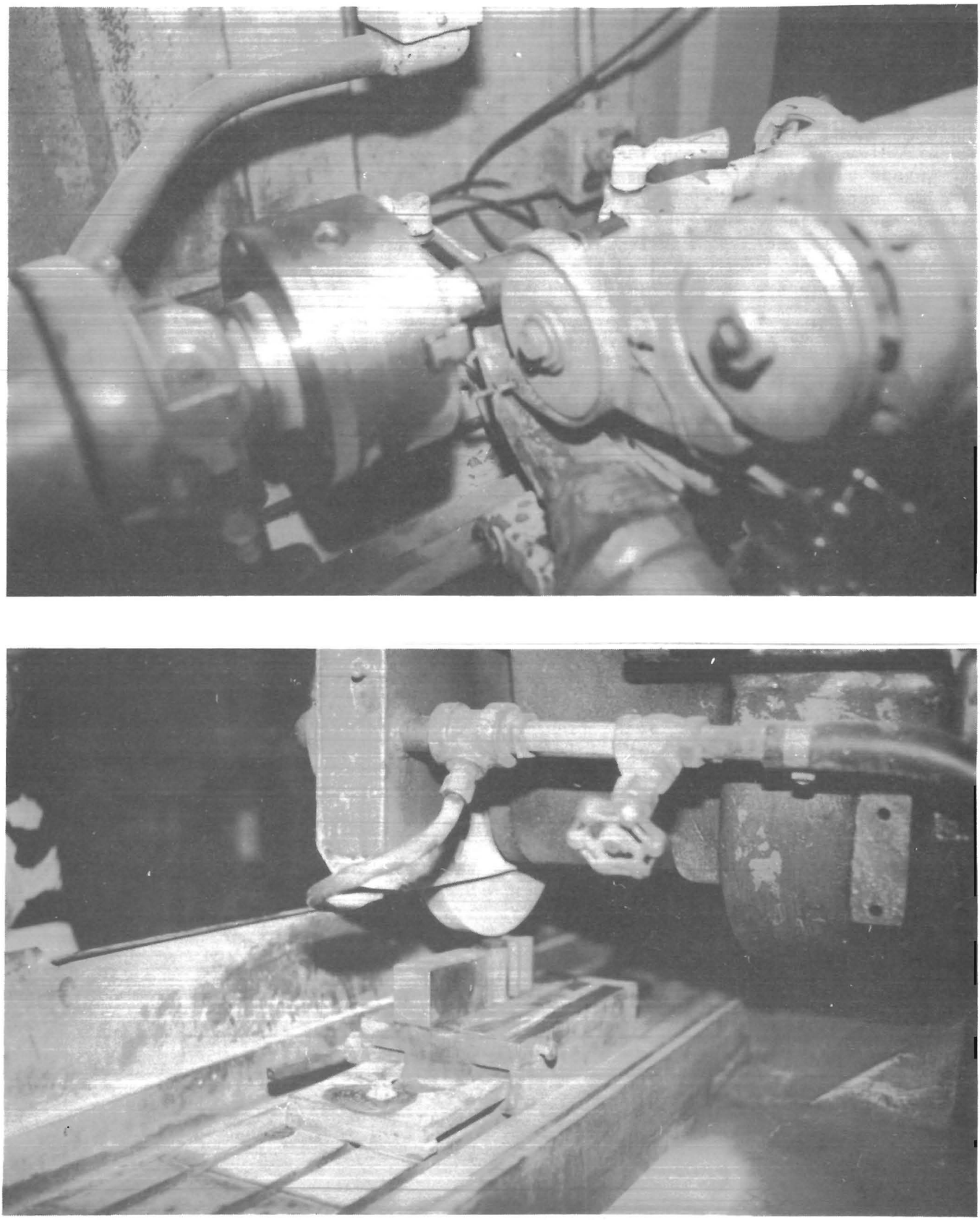

FIGURE 5.—Prismatic sample being turned in lathe to eliminate edges (top) and preparation of parallel ends of cylindrical samples in surface grinder (bottom).

TABLE 3. - Mechanical properties of dry seabed rock samples in comparison with properties coal and Icelandic hyaloclastites

Property	Manganese crust[1]	Hyalo-clastite[1]	Phospho-ritic rock[1]	Coal	Icelandic hyalo-clastite[2]
Density, g/cm^3:					
Bulk	1.31	1.58	1.91	NA	1.4-1.95
Solid	2.81	2.54	2.76	NA	NA
Shore hardness	18	9	15	NA	NA
Porosity, pct	55	38	32	NA	22-36.5
Void ratio	1.22	0.61	0.47	NA	NA
Compressive strength, MPa	8.36	3.66	32.55	[3]10.3-49.9	1.5-31.8
Tensile strength, MPa	1.75	NA	4.51	[3]0.61-17.78	0.3-2.7
Young's modulus, GPa	2.15	0.31	10.08	[3]2.7-3.35	0.4-6.9
Poisson's ratio, dynamic	NA	NA	NA	[4]0.37-0.44	0.17-0.28
Cohesive strength, MPa	2.9	NA	7.8	[4]1.4-4.4	0.52-0.53
Angle of internal friction, °	42	NA	52	[4]30-38	35-50
P-wave velocity, km/s	2.26	1.01	3.45	[4]2.0	NA

NA Not available.
[1]As reported by Cruickshank (1).
[2]As reported by Oddson (6).
[3]As reported by Evans (9).
[4]As reported by Calcott (8).

TABLE 4. - Mechanical properties of brine-saturated seabed rock samples

Property	Manganese crust[1]	Hyalo-clastite[2]	Phosphoritic rock (trachyte)[3]	Basalt[4]
Specific weight, g/cm^3	1.82-1.89	1.78-1.8	2.07-2.16	1.78-2.79
Shore hardness	9-12	3-4	12-25	56-57
Compressive strength, MPa	5.39-8.92	1.71-3.86	7.29-12.4	164.85-218.7
Tensile strength, MPa	[5]0.45	50.23	0.345-0.615	[5]11.86
Young's modulus, GPa	3.11-4.25	0.62-1.4	2.24-4.76	51.3-63.65
Poisson's ratio, dynamic	0.11-0.34	0.15-0.29	0.171-0.341	0.195-0.219
P-wave velocity, km/s	2.72-2.78	2.07-2.13	2.63-2.87	5.76-5.80
S-wave velocity, km/s	1.35-1.83	1.15-1.33	1.29-1.67	3.46-3.57

[1]Samples identified in appendix A as J and Y.
[2]Samples identified in appendix A as G and B.
[3]Samples identified in appendix A as D, U, and Y.
[4]Sample identified in appendix A as M.
[5]Obtained from 1 sample only.

and unconfined compressive strength tests. In the shear stress (τ) and normal stress (σ) coordinates, the cohesive strength was determined from the intercept of the tangent on the τ-axis (fig. 6). Likewise, the angle of internal friction was measured from the slope of the line tangent to the Mohr circles.

The mechanical properties of the brine-saturated samples are shown in table 4. The apparent wide range in strength properties for phosphoritic rock probably is due to variations in internal structure rather than the effect of brine on on the test samples. Such variations of the tensile strength, 0.35 to 0.62 MPa, and the compressive strength, 7.29 to 12.4 MPa, seem to depend on palagonitic nature of the crust as a result of volcanic activities and solidification processes similar to those forming several Icelandic hyaloclastites (6).

The mechanical properties of these geomaterials vary because they are very inhomogeneous. The inhomogeneity is discernible in macroscopic examination of the internal structure of the manganese crust and the phosphorite, and from the

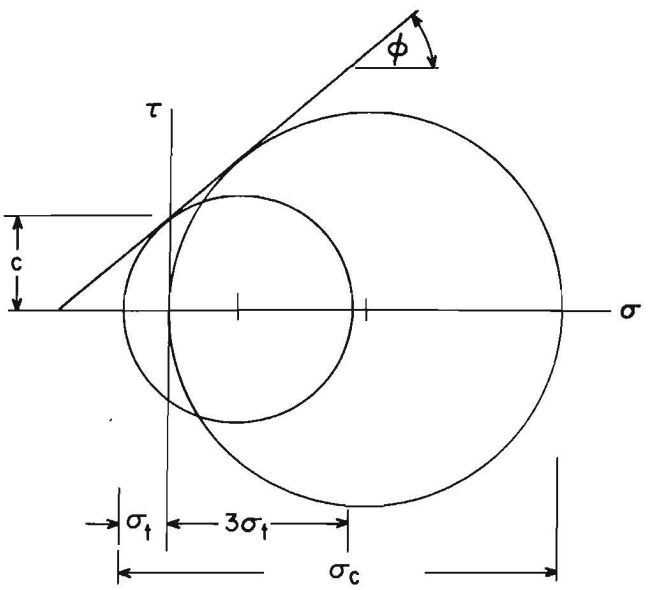

KEY

σ_t Tensile strength
σ_c Compressive strength
c Cohesive strength
ϕ Angle of internal friction
τ Shear stress
σ Normal stress

FIGURE 6.—Graphical determination of cohesive strength and angle of internal friction.

conglomerated structure of weak and strong rocks in hyaloclastite. The cohesive strength and angle of internal friction are presented in table 5.

Based on the engineering classification of Deere for intact rocks (7), which uses uniaxial compressive strength and the ratio of tangent modulus to strength, a comparison was made among the sea-floor materials (6), coal (8-9), and coal measure rocks (10) (fig. 7). The manganese crust is in the very low strength range and the sea-floor hyaloclastite is in the very low to low modulus ratio range near that of the Icelandic hyaloclastites. Phosphorite is in the same range as the manganese crust and hyloclastites. Basalt is of high strength, comparable to that of high-strength limestones.

Rippability

At present, there is no quantitative measure of rippability for rocks, except for a rough estimate in terms of the seismic velocity of soil-like excavation materials (11). For example, reference correlations indicate that a ground bucket wheel excavator could excavate rock that has a seismic velocity less than 1 km/s. For most rocks, the reliability of this scale has not been ascertained.

Based on mechanical properties, rippability can be more precisely determined from the cohesive strength and the angle of internal friction of the materials, using the cutting force equation derived by Nishimatsu (12) for drag bits. For 0° rake angle, the original equation is reduced to

TABLE 5. Cohesive strengths and angle of internal friction of seabed rocks

	σ_T, MPa	σ_c, MPa	ϕ, °	c, MPa
Manganese crust:				
Dry[1]	1.75	8.36	42	2.9
Saturated	.45	7.24	76	1.49
Hyaloclastite, saturated	.23	1.78	61	.4
Phosphoritic rock:				
Saturated	[2].48	[3]8.96	76.5	2.27
Dry[1]	4.51	32.55	52	7.8
Basalt, saturated	11.86	[2]191.78	76	26.42

σ_T Tensile strength.
σ_c Compressive strength.
ϕ Angle of internal friction.
c Compressive strength.

[1]Strength data from table 3.
[2]Average value of 2 samples.
[3]Average value of 5 samples.

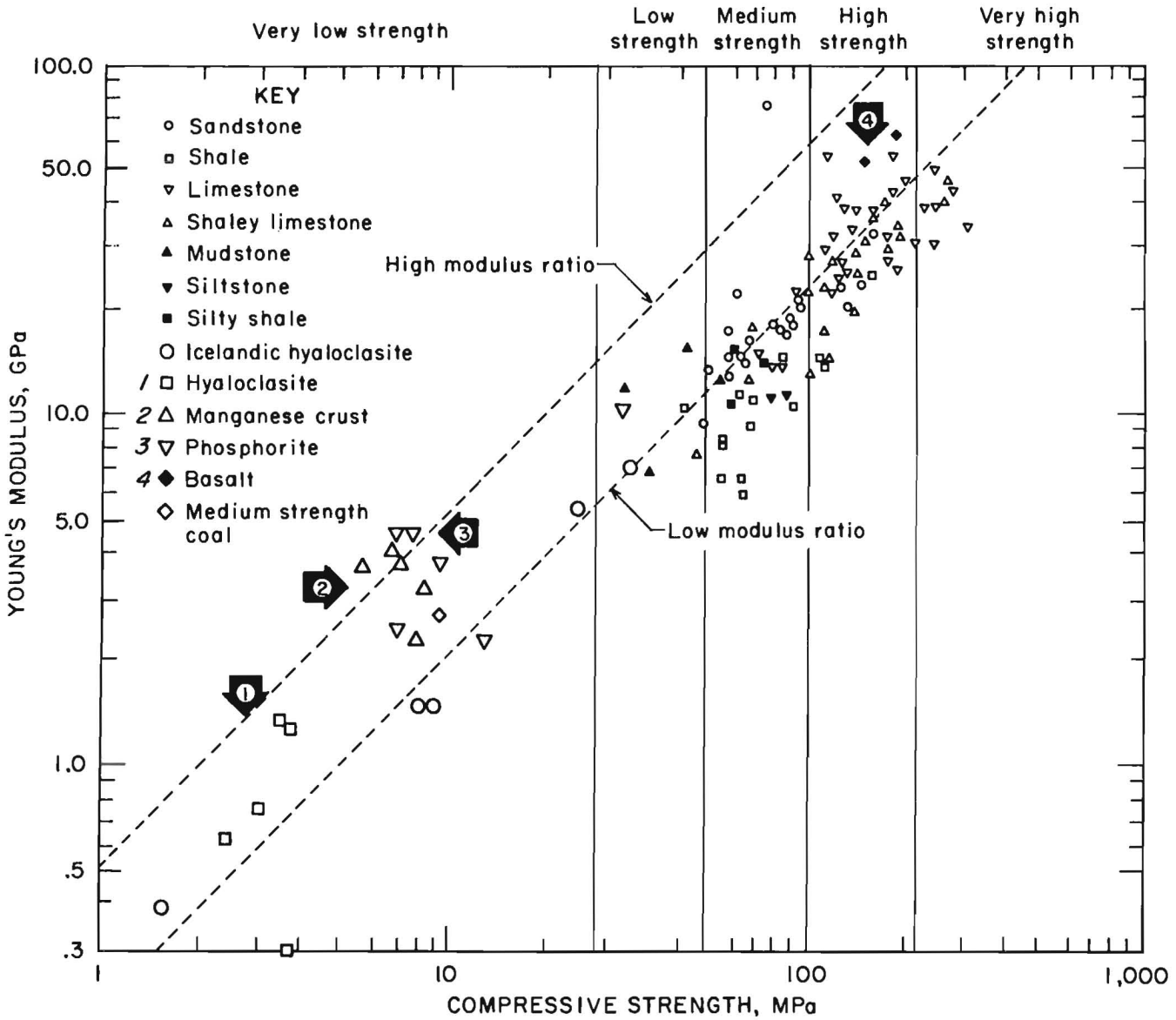

FIGURE 7.—Test data from tables 3 and 4 compared with data for coal and coal measure rocks.

$$\frac{F}{t} = \frac{c\ (\cos\Phi)}{6[1-\sin(\Phi+\beta)]}$$

where F is the cutting force per unit width, t is depth of cut, c is the cohesive strength, Φ is angle of internal friction, and β is the friction angle in cutting. This cutting angle is assumed to be 24° for the seabed materials and coal. The highest values of c and Φ were used in determining the force per unit area cut, F/t.

Comparative rippability indexes for the seabed rocks were determined by normalizing the calculated cutting force, F/t, to the value obtained for medium hard coal. This permits one to envision the feasibility of mechanically ripping the seabed materials at an acceptable production capacity (table 6). Because bituminous coal has been effectively produced in large scale by mechanical excavation, the rippability index for medium hard coal was defined as 1. Table 6

TABLE 6. - Rippability index (RI) of seabed rocks

	ϕ, °	c, MPa	F/t, MPa	RI
Medium hard coal.....	38	4.4	4.94	1.0
Manganese crust:				
Dry.....	42	2.9	4.18	.85
Saturated.....	76	1.01	2.69	.54
Hyaloclasite, saturated.....	61	.4	8.08	1.64
Phosphoritic rock:				
Saturated.....	76.5	2.27	5.19	1.05
Dry.....	52	7.8	26.69	5.4
Basalt, saturated.....	76	26.42	71.0	14.38

ϕ Angle of internal friction. F/t Force per unit area cut.
c Cohesive strength.

indicates the manganese crust would be easier to cut than medium hard coal. Hyaloclasite would be more difficult to cut than medium hard coal, but it would be technically viable. Phosphoritic rock and basalt require further consideration if they are to be mined simultaneously with the crust their rippability indexes are significantly higher than that of medium hard coal.

DISCUSSION

Seabed rocks are classified as weak rocks of low to very low strength, except for the basalt, based on a preliminary evaluation of a small quantity of samples. More sampling and environmental testing would be necessary to adequately represent the material properties under in situ conditions. Estimates of the rippability index derived for the manganese crust, from the cohesive strength and angle of internal friction, were made and compared with that of medium hard coal. Although the manganese crust itself appears to be easily rippable, the associated substrates, including some phosphorites, basalt, and some hyaloclastites, appear to be more difficult to excavate than even hard coal on these preliminary estimates.

Because the crusts and substrates of interest commonly occur at water depths of approximately 800 to 3,000 m, the hydrostatic pressure at such depth and pore pressure could be high enough to affect the strength of rocks. However, pressure effects were beyond the scope of the current study and would need to be examined in follow-on efforts. The variations in mechanical properties of the seabed rocks in tables 3 and 4 are due largely to the differences in the thickness of these crusts, nonhomogeneity in internal structure, and the site location of the dredged samples. The properties, therefore, are best defined statistically for each type of material. More sampling and testing is needed to obtain statistical confidence intervals that would permit application in selecting and designing appropriate mining equipment.

MECHANICAL CUTTING CHARACTERISTICS

SPECIMEN PREPARATION

All samples used in these cutting tests were kept immersed in seawater from the time of collection through the completion of testing. To reduce sample breakup and thereby maximize the number of cutting tests, the various sized and shaped samples were encased in hydrostone with only the surface to be cut exposed. These blocks were then secured in place by bolts and plates. A special watertight sample holder was constructed for these tests that allowed the cutting to take place under water. This holder was made of clear plexiglass for corrosion resistance and to allow the cutting action to be observed during the tests. Most samples were large enough to allow a cut length of 10- to 20-cm and two to eight

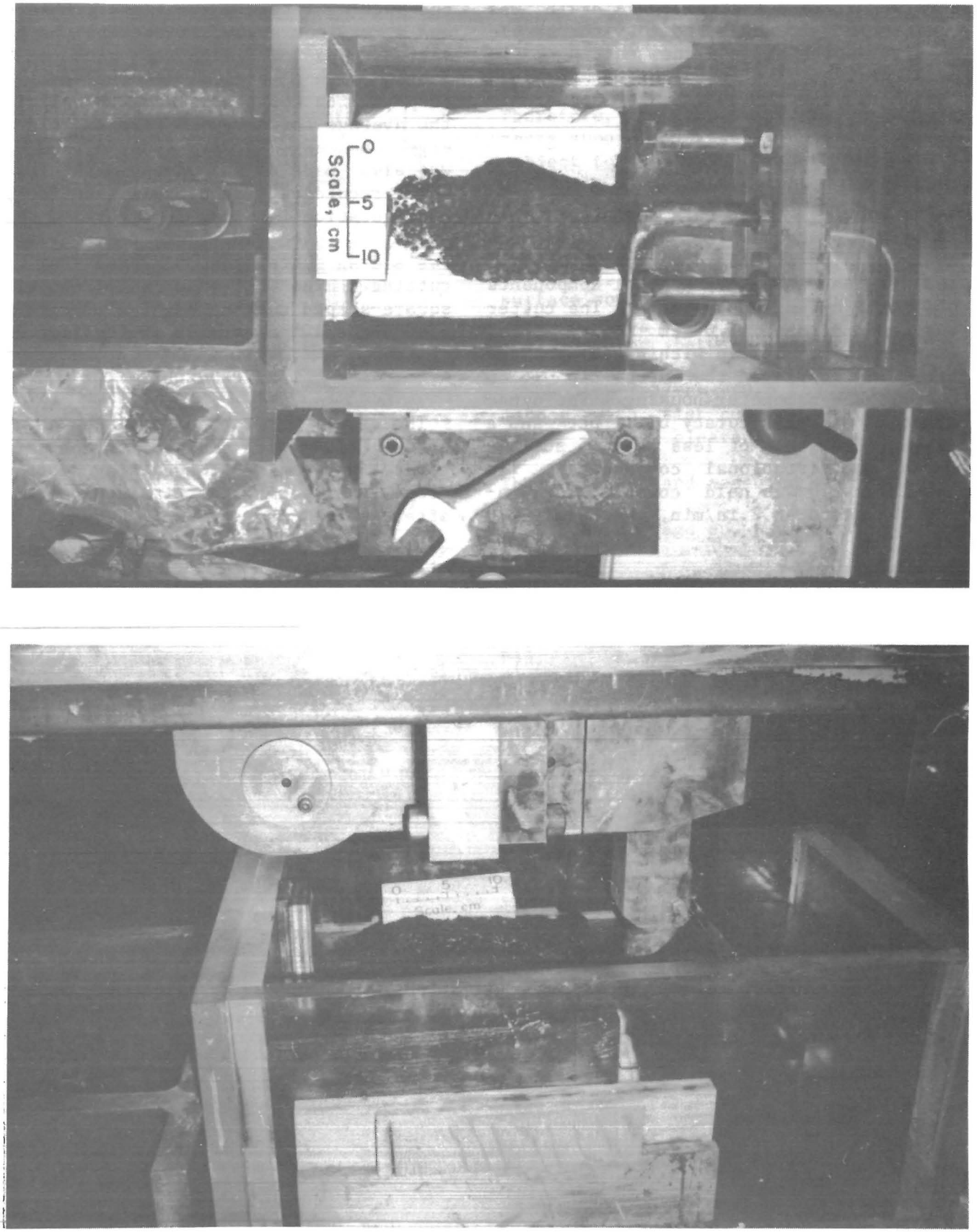

FIGURE 8.—Sample holder, top and side view.

separate cuts per sample. A drain was constructed in the bottom of the sample holder, which allowed the cuttings, including fines, to be collected for further analysis. The sample holder is shown in figure 8.

TEST APPARATUS

The cutting tests were performed on a converted planer mill. This mill was equipped with a three-axis dynamometer to measure the three orthogonal components of force acting on the bit. The cutter was mounted on a 5.08-cm square post, 25.4 cm long, clamped within the dynamometer, which placed the cutter tip 16 cm below the dynamometer housing. The dynamometer has an accuracy of ±1 pct and a maximum crosstalk of less than 5 pct between the orthogonal components. The cutting speed was held constant throughout the tests at 2 in/min, which allowed the cutting action to be closely observed and a maximum amount of data to be collected. The force data were gathered and stored with a digital storage oscilliscope, which was programmed to calculate the average forces, peak forces, and energy consumed. A hard copy of the data was also made on a conventional strip-chart recorder. The overall test faclity configuration is shown in figure 9.

The bit used for these cutting tests was a drag cutter commonly used for coal cutting. The bit had a 1/2-in wide, square-shaped cutting edge, a 0° rake angle, and a 10° clearance angle (fig. 10).

TEST PROCEDURE

The sample was locked in place and the holder filled with seawater to completely cover the sample. The cutting depth was preset by lowering the bit into position, after which the cutting sequence was

FIGURE 9.—Cutting test laboratory, milling machine in background and instrumentation in foreground.

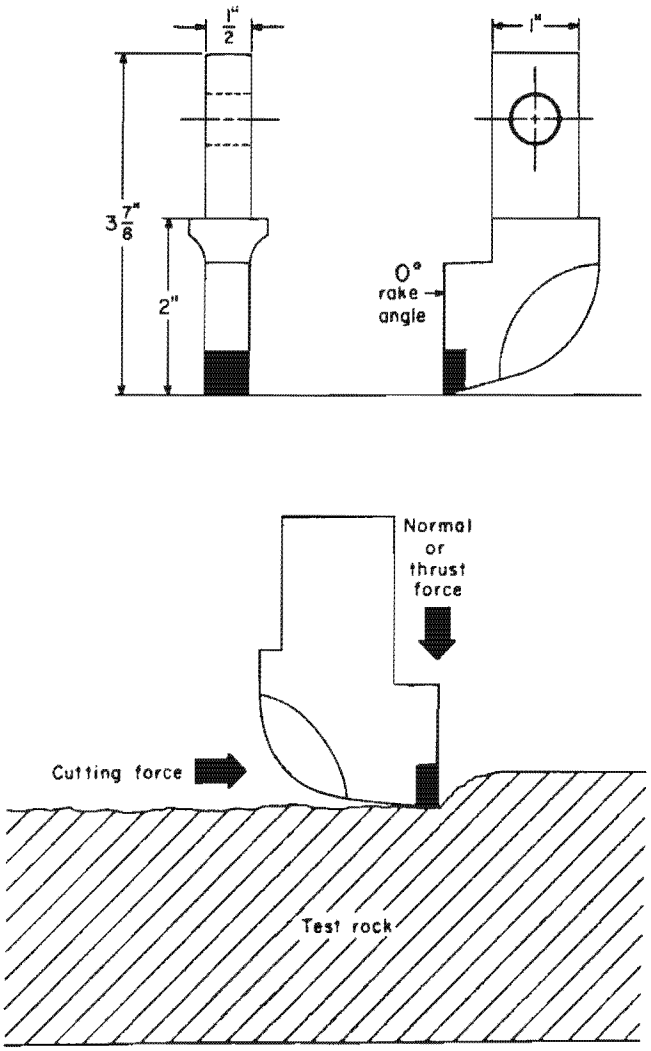

FIGURE 10.—Drag cutter used in cutting tests (top) and force convention used in analysis (bottom).

commenced by moving the bit across the sample. Both the crust and the substrate materials were cut during these tests.

Because the surface of the samples had a botryoidal texture and variable relief, the depth of cut actually varied throughout the cut from the preset depth. To aid in the analysis of the cutting data, the surface profile of each run was taken and recorded before each run. This allowed the depth of cut to be determined at any point along the cut. Adjacent cuts were spaced at various distances to determine the effect of cut spacing, on cutting performance. When the spacing-to-depth ratios were large, the cutting tests were independent of one another. At smaller ratios, called dependent cutting, chips broke to the free face within adjacent cuts.

Because of the limited number of samples available, little or no replication of individual cutting tests was possible. Therefore, the conclusions based on these tests should be viewed as preliminary and subject to change as more data become available. The independent variables are summarized as follows:

1. Cut depth--0.32, 0.64, 1.27, 2.54 cm preset, but varied because of surface roughness.
2. Cutting speed--5.08 cm/min.
3. Spacing between cuts--varied from 2.54 to 6.35 cm.
4. Bit--1.27-cm (0.5 in) wide, drag cutter, with flat cutting edge, 0° rake angle, and 10° clearance angle.

The dependent and measured variables were

1. The average and peak cutting force on the bit.
2. The average and peak normal forces on the bit.
3. The specific energy of cutting.
4. The size distribution of cuttings.

RESULTS AND DISCUSSION

Cutting Forces

The cutting and normal force data for all tests is given in appendix B and is summarized in table 7. A representative trace of a typical test is shown in figure 11 along with average force. The figure also shows the surface profile of the cut illustrating the variable depth of cut throughout the run. The force peaks in figure 11 coincide with the formation of chips ahead of the cutter and is typical of coal and rock cutting. The chipping action has highly influenced by the rock itself; the crust fractured along cracks, mud seams, and parting planes; and the very low strength substrates tended to kerf, leaving cores between adjacent tests.

The average cutting forces vary because of the changing cutting depth, but do generally show that cutting force is a

TABLE 7. - Summary of bit force and energy for 0° radial drag bit

	Depth of cut, cm			Cutting force, N			Normal force, N			Specific energy, J/cm³	
	Range		Av	Range		Av	Range		Av	Range	Av
	Av	Max		Av	Peak		Av	Peak			
CRUST											
I....	0.39-0.93	0.63-1.68	0.65	119- 694	565- 1,690	264	65- 141	141- 463	86	0.66- 2.22	1.48
D....	.50- .99	.64-1.27	.75	24- 373	314- 1,864	219	9- 278	69- 1,810	87	.01- 1.17	.82
I[1]...	1.19	1.57	1.19	476	1,619	476	136	583	136	.48	[2].48
D....	1.19-1.46	1.27-1.98	1.31	197- 810	725- 3,323	383	67- 391	430- 1,570	166	.04- 1.55	.43
I....	1.88-1.91	1.91-2.54	1.90	663-1,441	4,146- 4,319	1,052	278- 520	1,708- 1,810	399	.75- .78	.76
D[1]...	1.91	1.91	1.91	863	3,407	863	339	1,423	339	.33	.33
I[1]...	2.54	2.54	2.54	1,192	4,693	1,192	596	1,819	596	.14	.14
SUBSTRATE[3]											
C, D:											
I[1].	0.64	0.64	0.64	190	1,241	190	98	435	98	2.11	2.11
D..	.64	.64	.64	138- 297	569- 1,503	218	30- 133	181- 492	82	0.63- 1.24	.94
I[1].	1.28	1.28	1.28	890	4,426	890	224	885	224	1.85	1.85
F:											
D..	.64	.64	.64	159- 318	1,068- 1,219	238	50- 253	322- 1,125	152	.90- .94	.92
I[1].	1.27	1.27	1.27	395	1,708	395	33	176	33	1.35	1.35
G, I:											
D..	1.13-1.27	1.27-1.45	1.20	92- 225	774- 810	158	18- 41	145- 155	30	.24- .58	.41
D..	2.10-2.34	2.29-2.79	2.20	196- 395	364- 1,281	298	73- 95	160- 454	87	.03- .74	.29
I..	2.54	2.54	2.54	494-1,040	1,281- 1,713	778	92- 194	349- 396	129	.60- .83	.73
H:											
I[1].	1.18	1.78	1.18	122	511	122	42	330	42	.34	.34
D[1].	1.36	2.22	1.36	111	463	111	25	176	25	.16	.16
I[1].	1.60	1.91	1.60	247	1,188	247	64	416	64	.48	.48
J: I[1]	1.27	1.27	1.27	1,619	4,213	1,619	876	1,632	876	NA	NA
M:											
I[1].	.32	.32	.32	5,354	10,782	5,354	3,784	8,949	3,784	35.80	35.80
D..	.32	.32	.32	2,571-7,460	7,166-13,425	5,015	1,864-5,822	5,697-10,613	3,843	4.86- 6.72	5.79
Y: D[1]	2.54	2.54	2.54	6,303	12,570	6,303	2,793	5,587	2,793	1.00	1.00

I Independent. NA Not available. [2]Cuttings include large slabs of crust broken off end of cobble.
D Dependent. [1]Obtained from 1 test. [3]C-D, F-J, M, and Y refer to samples described in appendix A.

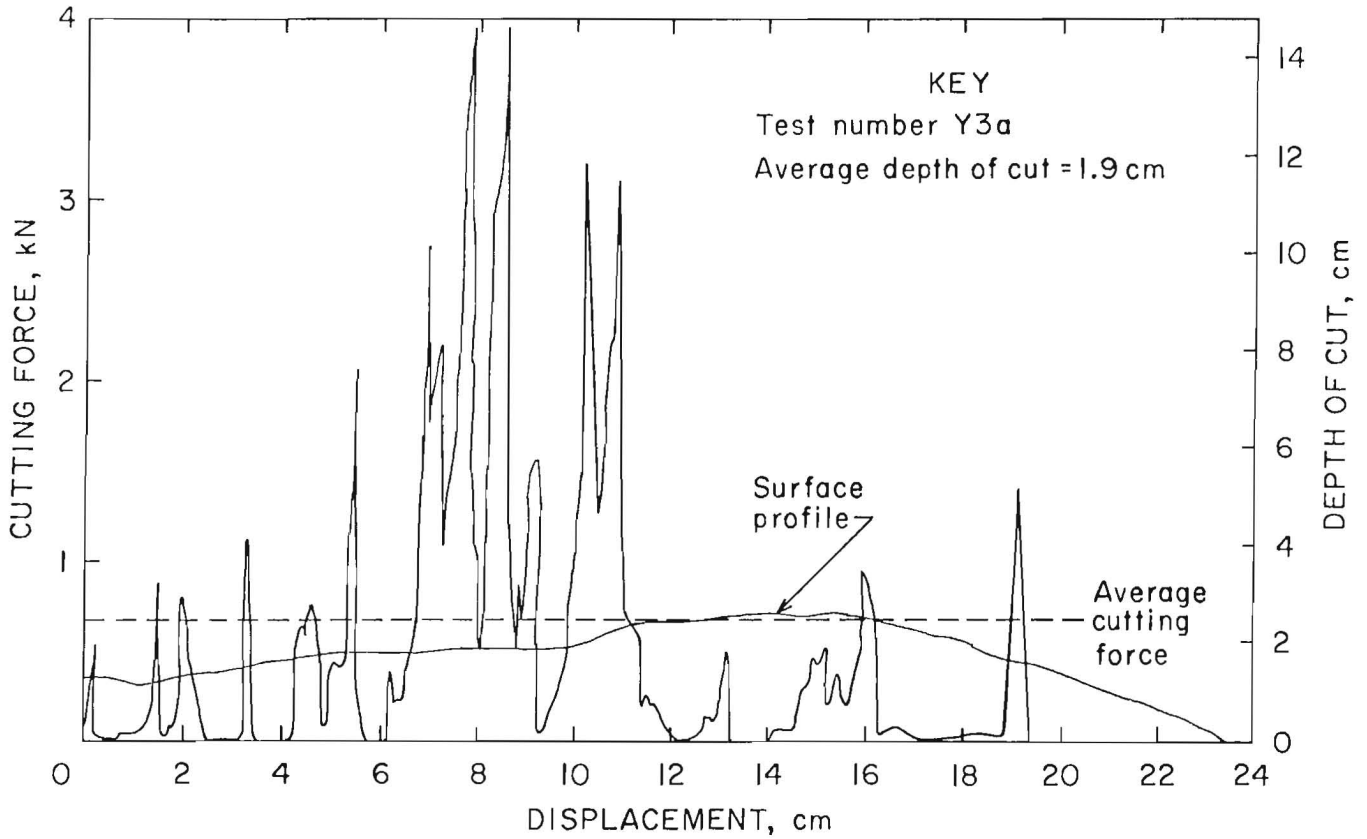

FIGURE 11.—Typical cutting force versus displacement for drag cutting tests.

a function of cutting depth. While the lack of uniform depth prevents a detailed analysis, the data indicate for crust and substrate that cutting force is approximately a linear function of cutting depth. When cutting crust and very low strength substrate (G, H, and I), a 2-cm depth of cut requires approximately twice the cutting force required for a 1-cm depth of cut. Furthermore, for the same rock types, dependent cutting required a 30 to 50 pct less same-depth-cutting force as independent cutting. Dependent cutting is defined as a condition where the material remaining in the space between the active cut and the adjacent completed cut breaks off automatically and continuously during the cutting process.

The normal force acting on the cut is also a function of the depth of cut, but is usually less sensitive than the cutting force. Thus, while the normal force also increases with depth of cut, it does so at a slower rate than the cutting force. In general, the tests show that average normal force is approximately 40 pct of the average cutting force. Instantaneously the normal force would frequently equal the cutting force and occasionally increased to twice the cutting force.

The data also show that the peak forces for both the cutting force and the normal force are from four to five times the average forces. The peak to average force ratios are typical of coal cutting, but greater than higher strength rock cutting. The variation in peak forces was similar for both the crust and the substrate materials except for the higher strength trachyte (Y) and basalt (M). However, particularly in crust cutting, fractures were observed at significant distances in front of the cutter; thus after chip release the forces dropped to near zero values and remained there for unusually long periods of time. Note that mechanical cutting systems must be designed to supply the peak force to the bit and not the average force.

Besides the depth of cut, the bit forces are a function of the material being cut. Therefore, they will be different for both the crust and the substrate materials. At 0.75-cm depth of cut, the low strength substrates, C and D, required approximately the same cutting force as the crust; however, the very low strength substrate, G, I, and H, required in the order of one-half the 200-N force. At 1.5-cm depth, the low strength substrate required nearly twice the cutting force as the crust (650 N); whereas, the very low strength substrate required around one-third. At 2.5-cm depth, the very low strength substrate required approximately one-third the cutting force necessary for the crust (1 kN); however, the low strength trachyte, Y, needed approximately six times that force. The high strength basalt (M) required in the order of 50 times the cutting force necessary for crust cutting. This indicates the low- and high-strength substrate materials, especially the trachyte and basalt, will be substantially more difficult to cut than the crust. More tests must be conducted before this difference can be quantified, however.

The side forces experienced by the bit were low, as expected. For 90 pct of the tests, a peak value of 750 N was not exceeded. The independent cuts experienced a side-to-side force fluctuation of approximately equal value and the dependent cuts experienced forces predominantly towards the free face side. The side forces experienced are within normal values and should not be of major concern in any conventional mechanical cutting system.

Finally, the relative magnitude of the cutting, and the normal and side forces experienced during crust cutting are roughly comparable to coal cutting. The forces generated during the substrate cutting varied, with the very low strength altered basalt, G, I, and H, requiring low forces and low strength altered basalt, C and D, producing slightly higher forces, while the trachyte, Y, and basalt, M, produced the highest forces. In general, however, crust cutting itself is a comparatively easy cutting situation and the coal cutter used was adequate for the task. The only difficulty would be the trachyte, Y, and the basalt, M, which are reasonably strong and could tax coal cutting equipment if large amounts were encountered.

Specific Energy

The specific energy of a material is defined as the energy required to fragment a unit volume of the material. For drag cutting, the energy consumed is calculated by multiplying the average cutting force by the length of cut, and the volume is calculated by weighing the cuttings and converting to volume. The specific energy required to fragment both the crust and the substrates have units of joules per cubic centimeter. The data show that the specific energy varies for each sample tested, for each depth of cut, for each spacing, and whether crust or substrate material was cut. The specific energies in table 7 generally varied, similar to results from other rock cutting tests. Specific energies decreased as depth of cut increased and when comparing dependent to independent cutting. Average specific energy ranged as follows:

Crust cutting--0.14 to 1.48 J/cm^3.

Very low strength altered basalt, G, I, and H--0.16 to 0.73 J/cm^3.

Low strength altered basalt, C and D, trachyte--0.94 to 2.11 J/cm^3.

High strength basalt, M--5.79 to 35.80 J/cm^3.

For comparison, the specific energy range for coal under similar conditions is 2.0 to 2.7 J/cm^3 (13). Thus, generally the crust and low strength substrate material specific energy requirement is similar to coal, and coal cutting technology (bits and cutterheads) appear suitable for these types of deposits.

Size Analysis of Cuttings

The size of the cuttings produced by drag cutting depends primarily on the

TABLE 8. - Sieve analysis of manganese crust cuttings with 1/2-in drag cutter at 1.88- to 2.54-cm depth of cut, cumulative weight retainted, percent

Sieve size[1]	
2-1/2 in	34
2 in	61
1-1/2 in	63
3/4 in	72
3/8 in	81
4 mesh	89
8 mesh	93
16 mesh	95
30 mesh	97
50 mesh	98
100 mesh	99

[1]U.S. standard sieve series.

depth of cut and the spacing between cuts. Generally the deeper the cut, the larger the cuttings obtained. Similarly, there is an optium spacing between cuts that will also yield the largest size product. In all cases, however, the size of cuttings obtained from drag cutters will vary over a wide range, typically from 400 mesh and below to 1 in or more.

To obtain a representative sample of cuttings, the product from several runs made in the same sample were sized together. The size distribution for these collected cuttings is shown in table 8 and is typical for drag cutting. All screening was done wet to avoid further comminution of the fragile crust material. The data show that 1 pct of the cuttings are less than 100 mesh.

Because the fine particles can be difficult to collect under water, a representative sample placed in a graduated cylinder containing seawater was agitated, and the time to settle was observed. After 1 h, the smallest fines were still in suspension. These fines would be difficult to collect in an underwater mining operation and should be minimized as much as possible during cutting. It is estimated that these suspended fines will represent less than 1 pct of the total cuttings produced.

CONCLUSIONS

The results obtained from this study of cobalt-rich manganese crusts are in substantial agreement with those reported by other researchers (1). The crust varied in thickness from less than 1 mm to more than 3 cm with an average of 1 to 2 cm. The average cobalt content of the crust was about 1 pct and the average manganese content varied from 22 to 30 pct. The subtrate material was identified as unaltered and altered basalt and trachyte.

The physical properties confirmed earlier data that showed the crust itself to be a relatively weak material. The tensile and compressive strengths of the saturated crust were 0.45 MPa and 5 to 9 MPa, respectively. The substrate materials were more variable, with the trachyte having compressive strengths of 7 to 12 MPa, the altered basalt (hyaloclastite) having a compressive strength range of 2 to 4 MPa, and basalt having a compressive strength ranging from 165 to 219 MPa. The Shore hardness values of 9 to 12 for the crust is also indicative of a weak material. Finally, the dry bulk density of the crust material of 1.3 g/cm^3 and a porosity of 55 pct indicate a lightweight, porous material.

The mechanical cutting tests also show that the crust material is soft and easy to cut. Only selected samples of the trachyte substrate represent moderate cutting difficulty, and the unaltered basalt was extremely difficult to cut. The range of specific average energy required to fragment crust was 0.14 to 1.48 J/cm^3, which is in the same range as coal or other soft materials. The cutting forces required for the crust are also low, with an average cutting force requirement at a 2-cm depth of cut of 1 kN, and a peak force requirement of 4 to 5 kN. It is concluded that radial drag cutters designed for coal are adequate for crust cutting.

Finally, the reader is advised that although the tests tend to confirm previous results, the crust samples were stored in seawater for approximately 1 yr prior to testing. This long storage time may have caused some deterioration of the samples and could, therefore, have affected both the physical properties and the cutting

strengths. In addition, the limited number of samples minimized the number of tests and replications that could be conducted. Therefore, the data contained in this report should be considered preliminary and subject to change as more data become available.

REFERENCES

1. Cruickshank, M. J., and R. C. Paul. Characterization of Seabed Rocks for Mine Planning in the EEZ. Paper in Offshore Technology Conference 5236. Program Dep., Offshore Technol. Conf. (Richardson, TX) 1986, pp. 135-138.

2. Latimer, J. P., and R. Kaufman. Preliminary Considerations for the Design of Cobalt Crust Mining Systems in the U.S. Exclusive Economic Zone. Paper in Oceans 85. IEEE, 1985, pp. 378-399.

3. Johnson, C. J., A. L. Clark, J. M. Otto, D. K. Pak, K. T. M. Johnson, and C. L. Morgan. Resource Assessment of Cobalt-Rich Ferromanganese Crusts in the Hawaiian Archipelago. Resour. Systems Inst., East-West Center, Honolulu, Hawaii, May 1985, 49 pp.

4. Haynes, B. W., S. L. Law, and D. C. Barron. Mineralogical and Elemental Description of Pacific Manganese Nodules. BuMines IC 8906, 1982, 60 pp.

5. Lewis W. E., and S. Tandanand (eds.). Bureau of Mines Test Procedures for Rocks. BuMines IC 8628, 1974, 223 pp.

6. Oddsson, B. Engineering Properties of Some Weak Icelandic Volcanic Rocks. Paper in Weak Rock: Soft, Fractured and Weathered Rock (Proc. Int. Symp. on Weak Rock, Tokyo, Japan, Sept. 21-24, 1981). Balkema (Rotterdam), 1981, pp. 197-204.

7. Deere, D. U. Geological Considerations. Ch. 1 in Rock Mechanics in Engineering Practice, ed. by K. G. Stagg and O. C. Zienkiewicz. Wiley, 1968, pp. 1-20.

8. Calcott, T. C., and G. B. Smith. Mechnical Properties of Coal: Ch. 5 in Chemistry of Coal Investigation. Second Supplementary Volume, ed. by M. A. Elliot. Wiley, 1981, pp. 285-315.

9. Evans, I., and C. D. Pomeroy. The Strength Fracture and Workability of Coal. Pergamon, 1966, 277 pp.

10. Thill, R. E., and J. A. Jessop. Engineering Properities of Coal Measure Rocks. Soc. Min. Eng. AIME Preprint. 82-146, 1982, 9 pp.

11. Bell, F. J. Open Excavation. Ch. 17 in Foundation Engineering in Difficult Ground. Butterworth (Boston). 1978, pp. 513-538.

12. Nishimatsu, Y. The Mechanics of Rock Cutting. Int. J. Rock Mech. Min. Sci., v. 9, 1972, pp. 261-270.

13. Roepke, W. W., and J. I. Voltz. Coal-Cutting Forces and Primary Dust Generation Using Radial Gage Cutter. BuMines RI 8800, 1983, 24 pp.

14. Hein, J. R., F. T. Manheim, W. C. Schwab, and A. S. Davis. Ferromanganese Crusts From Necker Ridge, Horizon Guyot, and S. P. Lee Guyt: Geological Considerations. Mar. Geol., 1985, v. 69, pp. 25-54.

15. Burns, R. G. (ed.). Mineralogical Society Association Short Course Notes. Mar. Miner., v. 6, 1979, pp. 1-46.

APPENDIX A.--DESCRIPTION OF SAMPLES

Cross sections of representative samples are shown in figures A-1 through A-8.

Manganese Crusts.--Optical microscopic examination of the pavement in polished thin section reveals that the crusts are composed of small, scattered botryoids that nucleated on the substrate and eventually coalesced to form concentric or parallel layers as the crust continued to develop. Goethite and clay occur between layers and in fractures and open spaces between botryoids. A small amount of phosphate and silicate was found in the crusts; however, there were no concentrations of phosphates in the suite examined. Other researchers have reported discrete phosphate layers in the manganese crust and have ascribed some of the silicate content to fine, windblown dust from Asia (14).[1] All X-ray diffraction patterns of the crusts were similar, showing the presence of vernadite (delta-MnO_2) and varying amounts of goethite, which is identical to the results of other researchers (4, 15).

Substrates.--The trachytic substrates consisted mostly of subparallel lathes of sanidine (50 to 85 pct by volume) in a glassy matrix. Interspersed in this were small grains of hematite and secondary apatite filling voids between crystals of sanidine. Phillipsite occurred in these rocks, but mostly as secondary layer on the surface of the rock, or as a fracture or void filling.

The basalt substrates were more complex and variable. Brecciation of the volcanic substrate and crust, along with deposition of volcanic and organic sediment further complicated the rock texture. Most of the basalt was vesicular (almost spongelike) and in many of the samples the volume of pores or vesicles was high (up to 60 pct by volume).

Terms commonly used for these rocks are hyaloclastite and, with subsequent alteration, palagonite. The major mineral in the original rock was augite, occurring as subparallel to radiating lathes in a glassy matrix. Large altered euhedral olivine grains and skeletal hematite occurred throughout the matrix. The altered matrix was composed predominately of iron silica glass. One sample was an altered vitric tuff showing the typical glass shard texture with almost no crystalline phases.

The major secondary minerals were phillipsite and nontronite. Phillipsite occurred as botryoidal crusts and radiating crystals, filling vesicles and open spaces between fragments of altered basalt, manganese crust, and sediment. Nontronite directly replaced the basalt and occurred as brown to green radiating fibers and spherulites.

DESCRIPTIONS OF INDIVIDUAL MANGANESE PAVEMENT SAMPLES

Sample B.--Thick (3 cm) manganese oxide crust surrounding and covering rounded, irregular zones of yellowish to orange-brown altered basalt. Individual areas show color zoning: light yellow or white on the edge, dark orange to brown in the interior. The basalt is very porous, with a large percentage of rounded vesicles. Ragged, columnar augite crystals occur in an altered iron-rich silicate matrix. Massive phillipsite occurs, preserving the original outline and gross texture of the basalt, while radiating crusts of phillipsite fill vesicles. Botryoidal goethite occurs, usually separate from the manganese oxide crust.

Sample C.--Few small pieces (0.1-0.2 cm) of manganese oxide crust. Small piece of a highly altered breccia of basalt and some sediment, with goethite, manganese oxide, and hematite rimming of vesicles. Some carbonate rock fragments were found on one edge.

Sample D.--Thin to thick (0.2-1.5 cm) manganese oxide crust covering a breccia of highly altered basalt. White to transparent botryoidal layers (0.2- to 0.8-mm thick) of phillipsite rim the basalt and serve as the interface between the manganese oxide and the substrate. Green to brown spherulites of nontronite

[1] Underlined numbers in parentheses refer to items in the list of references preceding this appendix.

replace the basalt and fill vesicles. The overall rock texture appears sponge-like. Euhedral crystal outlines of altered olivines, 0.2 to 0.4 mm in diameter, are noted in the basalt.

Sample F.--Vesicular basalt containing fine (0.5-0.2 mm) subparallel to radiating augite crystals, skeletal ilmenite-hematite and phenocrysts of partially altered olivines (0.2- to 1.0-mm diam). Radiating phillipsite crystals rim vesicles and fill open spaces. Shell fragments and carbonate cement occur along one edge. Manganese oxide crust is very thin or absent (0.1 cm or less).

Sample G.--Large (5 by 8 cm) cobble of altered basalt with a thin (0.2 cm) manganese oxide crust layer on one side and a thick (1.5 cm) layer on the other. The cobble is yellow with irregular, patchy, orange to brown areas. The original vesicular texture has been preserved while being almost completely replaced by hematite, clay, and oolites of phillipsite. Some rock remnants similar to sample F remain.

Sample H.--Thick (3 cm) manganese oxide crust covering a brownish, iron-stained clay that was originally a basalt similar to the other rocks from this location.

Sample I.--Very thick (>3 cm) piece of manganese oxide crust. Trace of sediment and altered basalt, similar to sample G.

Sample J.--Very thick (>3 cm) manganese oxide crust covering a breccia composed of yellow to white altered vitric tuff and small pieces of manganese oxide crust. Clusters of large, twinned phillipsite crystals have filled in the open spaces and some fractures. Sediment of mineral fragments and clay fill the rest of the open space. Veinlets and fine dendrites of botryoidal manganese oxide are noted within the tuff. Some goethite occurs interlayered with the manganese oxides and in veinlets or separate botroidal zones.

Sample K.--Sediment composed of two distinct layers: A fine greenish-brown clay and a slightly coarser partially consolidated brown sediment. A thin (0.2 cm) manganese oxide crust coats the clayey layer. Both sediments are composed of volcanic rock fragments and organic remains. Broken and rounded crystals of plagioclase, pyroxene, and olivine occur in coarse lenses. Manganese oxide dendrites, hematite, and magnetite are also noted in the sediments.

Sample L.--Three different materials. One is breccia, with a thin to moderate (0.2-1.0 cm) manganese oxide crust. The orange-brown basalt fragments are angular to subrounded, showing a bleached alteration zone near the edges. Phillipsite fills fractures and open spaces between the breccia particles. The basalt is primarily composed of felted plagioclase and altered, iron-rich glass. Minor hematite occurs. Second is a thick (3 cm) manganese oxide crust. Third is a bleached yellow to white organic sediment, with a small amount of carbonate filling shells, and a thin (0.4 cm) manganese oxide crust covering it.

Sample M.--Large, irregular cobble (4 by 12 cm) of dark gray basalt, rimmed by four zones. The inner zone, next to the basalt, is a thin, light gray alteration zone. The next is a thin, brown, oxidized zone. A thin, white to yellowish layer of phillipsite partially rims the cobble. Finally, a manganese oxide crust forms the outer zone; a thin (0.1 cm) crust covering one side and a thick (1.0 cm) manganese oxide crust covering the opposite side.

Sample N.--Very thick (>3 cm) manganese oxide crust on a very small piece of grayish sediment and altered basalt substrate. Phillipsite occurs as a void filling.

Sample O.--Greenish trachytic sanidinite cobble, similar to sample T, with thin to medium (0.2-1.5 cm) maganese oxide crust. Some phillipsite and sediment attached on one side.

Sample S.--Thick (2.0 cm) manganese oxide crust on a poorly consolidated gray sediment of sand and silt particles.

Sample T.--White to patchy greenish trachytic sanidinite cobble covered by a thin (0.2 cm) manganese oxide crust on one side and a thick (2.0 cm) manganese oxide crust on the opposite side. The rock is composed of essentially sanidine (parallel flow texture) with minor hematite, in a glassy matrix that is partially replaced by apatite. The thicker crust zone is actually a breccia of trachyte and organic sediment surrounded by manganese oxide crust with some goethite rimming the manganese oxide botyroids.

Sample U.--Greenish trachytic sanidinite cobble, similar to sample T, covered by very thin (<0.2 cm) manganese oxide crust.

Sample X.--Grayish green trachytic sanidinite cobble, similar to sample T, covered by thin to very thin (0.2-<0.1 cm) manganese oxide crust on one side and a brecciated mixture of manganese oxide crust and trachyte pebbles with a matrix of yellowish white, massive, porous phillipsite on the opposite side.

Sample Y.--Very thick (>3 cm) manganese oxide crust with small amount of breccia attached to grayish green trachytic sanidinite cobble, similar to sample T.

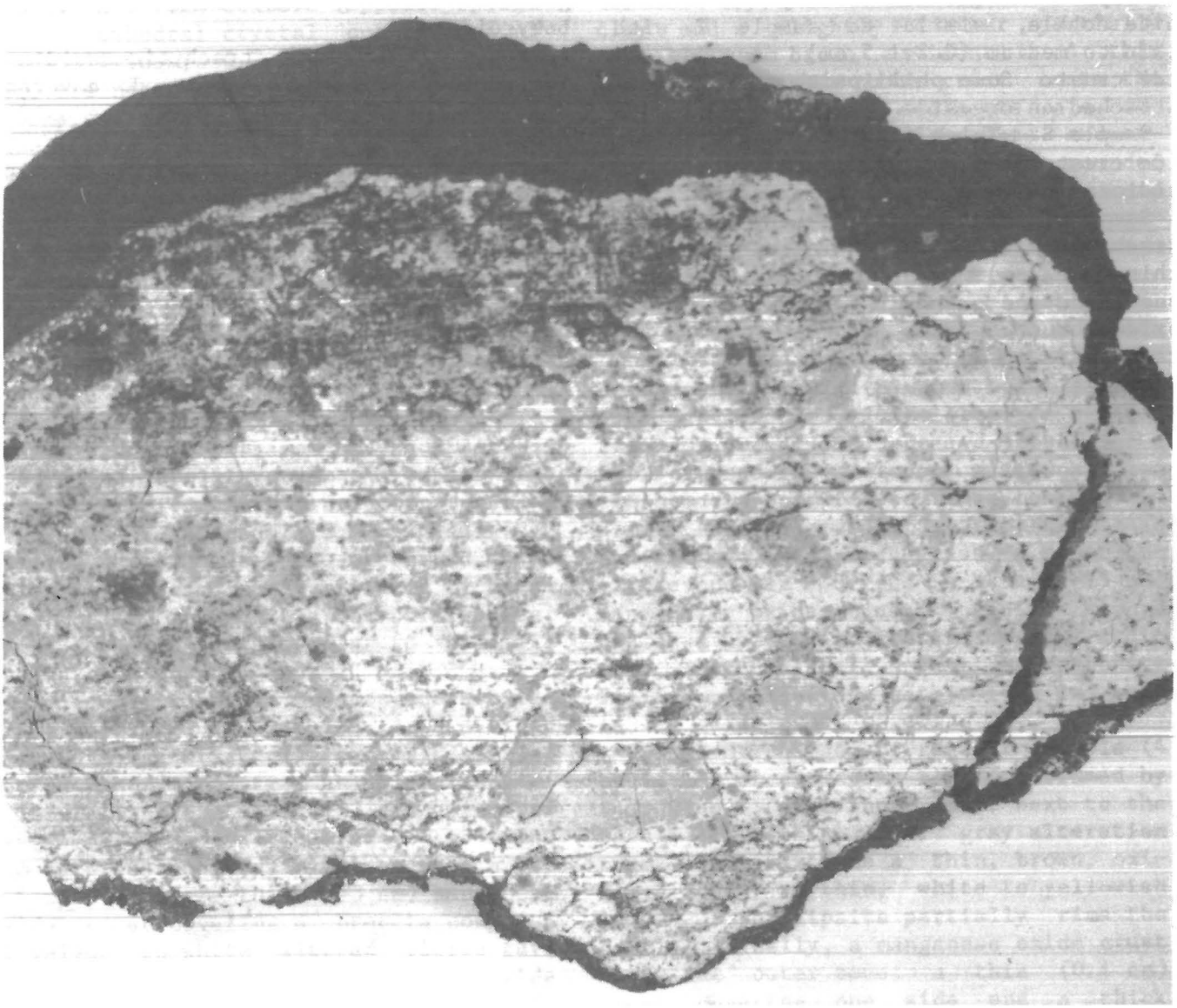

FIGURE A-1.—Sample G cross section (X 1). Manganese crust coating highly altered basalt cobble. (Note rapid thinning of crust at median line and difference in thickness of crust between top and bottom of cobble.)

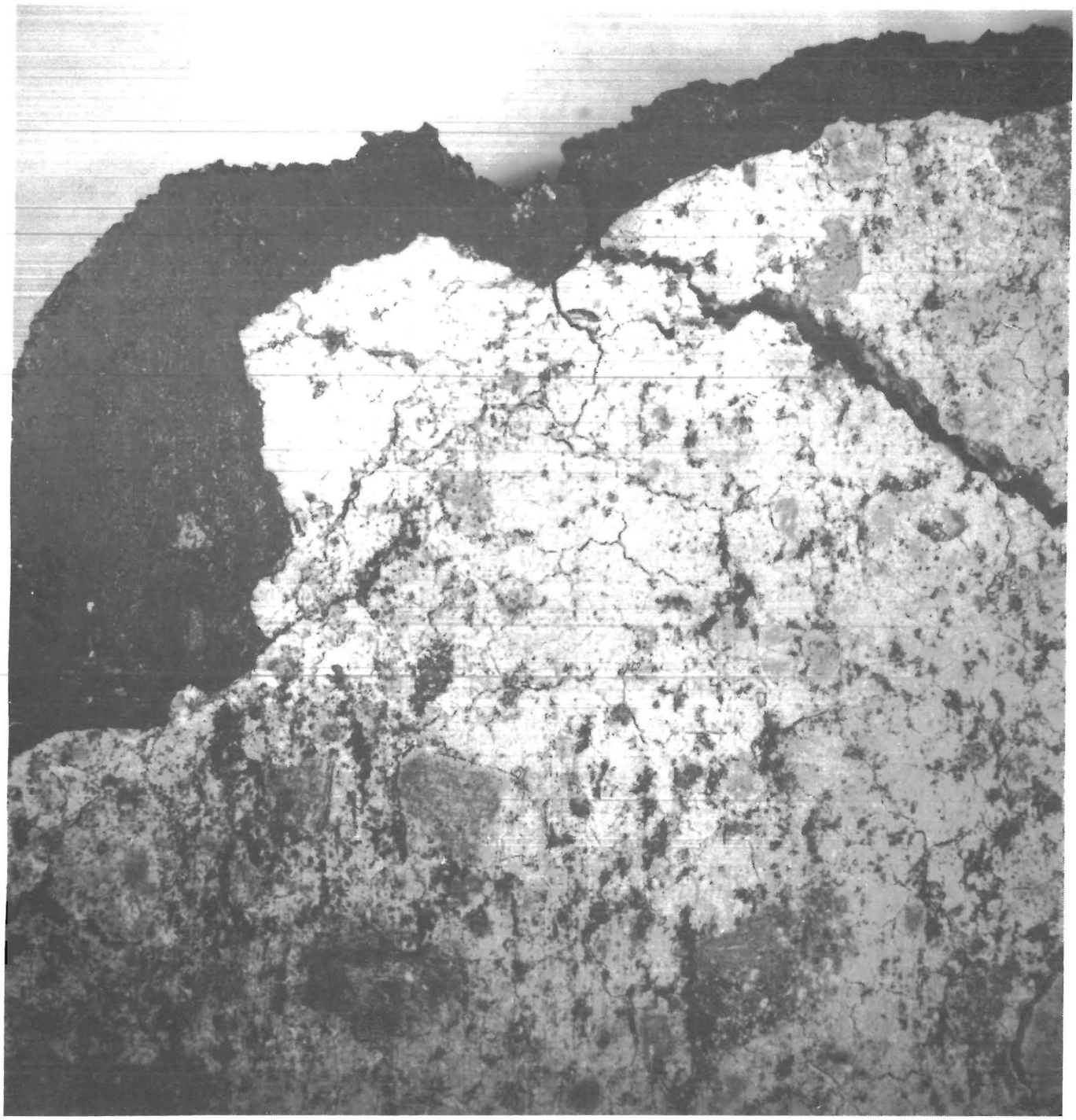

FIGURE A-2.—Sample G cross section (X 3). Texture and subsequent fracturing after air drying at room temperature Both rock and crust are very friable.

FIGURE A-3.—Sample M cross section (X 1). Manganese crust coating basalt cobble. (Note thickness difference similar to sample G.)

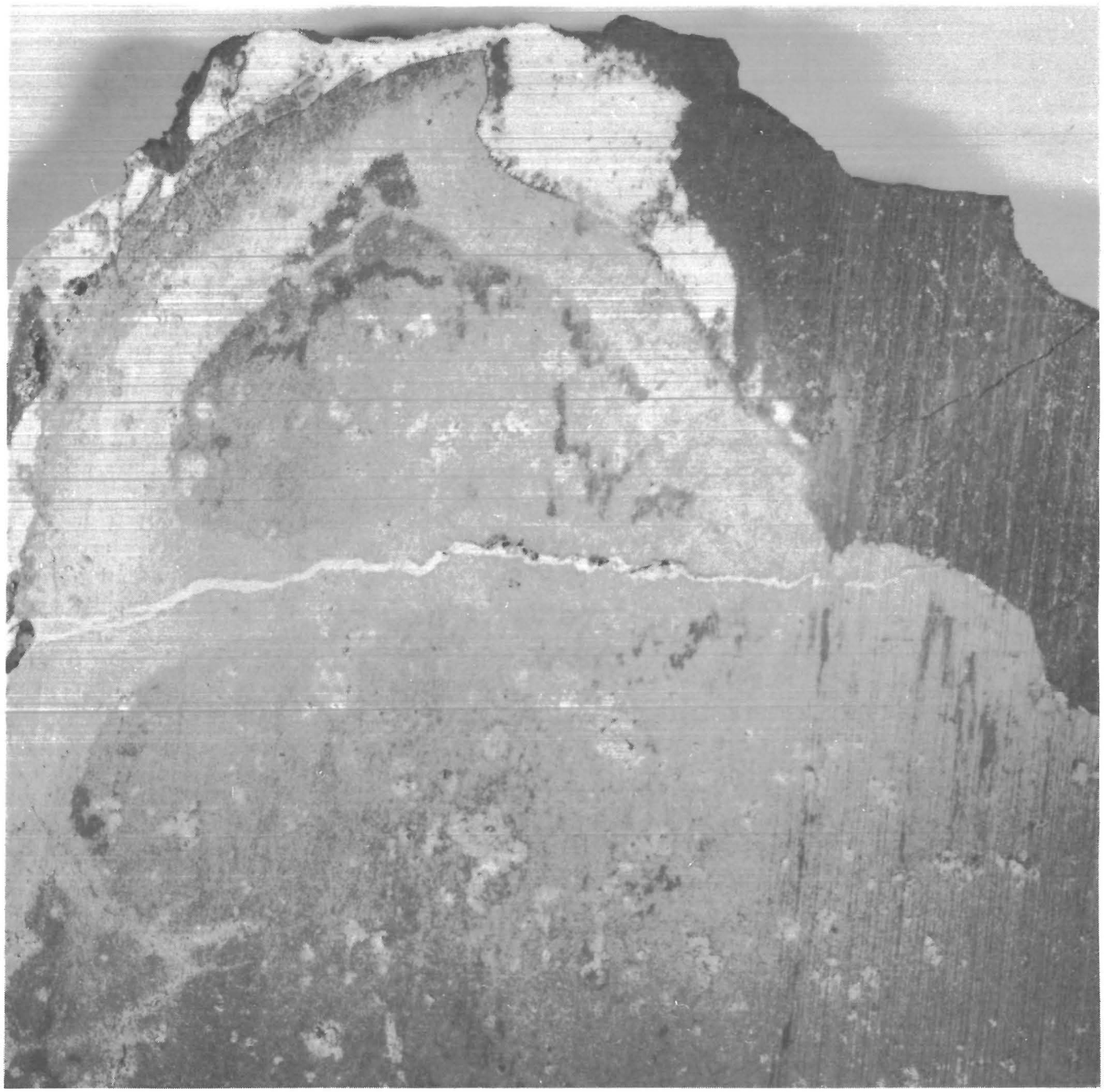

FIGURE A-4.—Sample M cross section (X 3). After air drying at room temperature, rock is still competent, however, manganese crust is fractured and very friable.

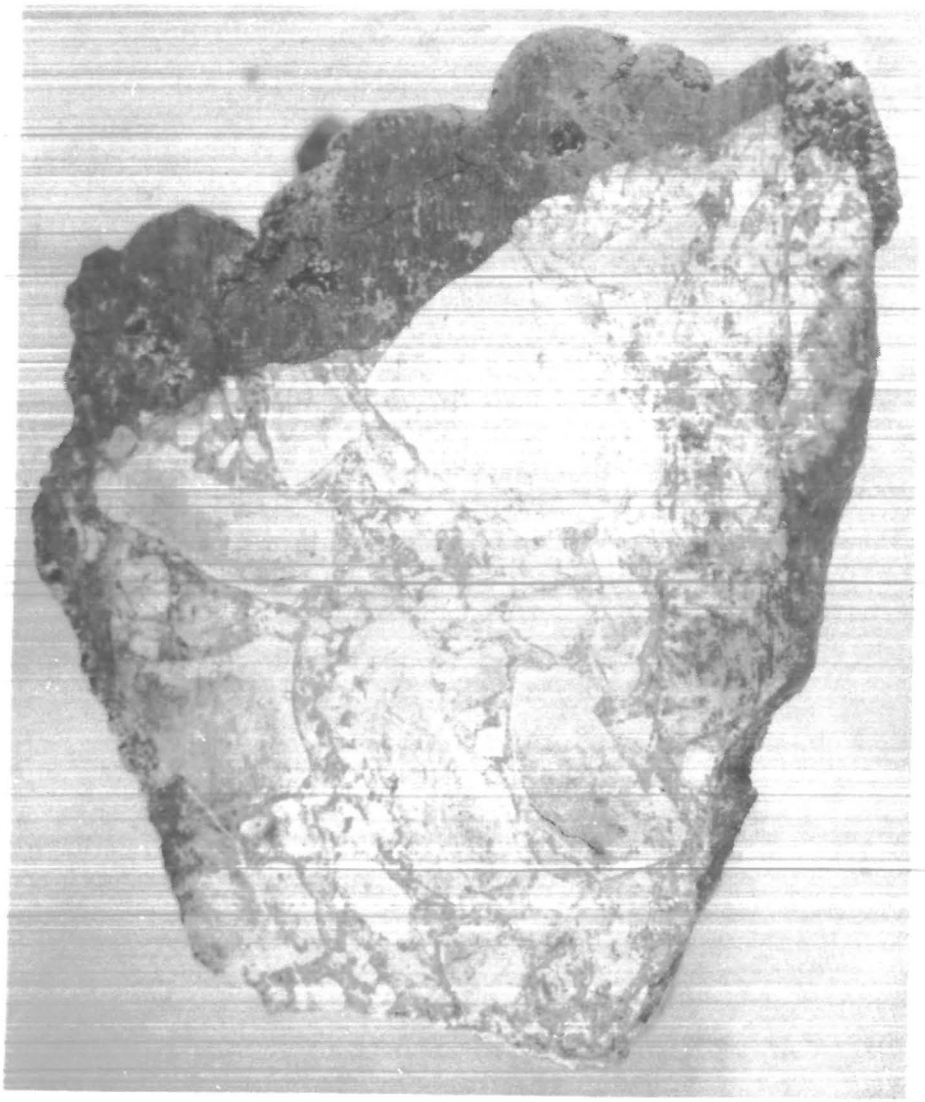

FIGURE A-5.—Sample K cross section (X 3). Altered basalt breccia covered by manganese crust.

FIGURE A-6.—Sample D cross section (X 3). Substrate is altered basalt breccia, partially replaced by nontronite and encrusted with white to transparent layers of botryoidal phillipsite.

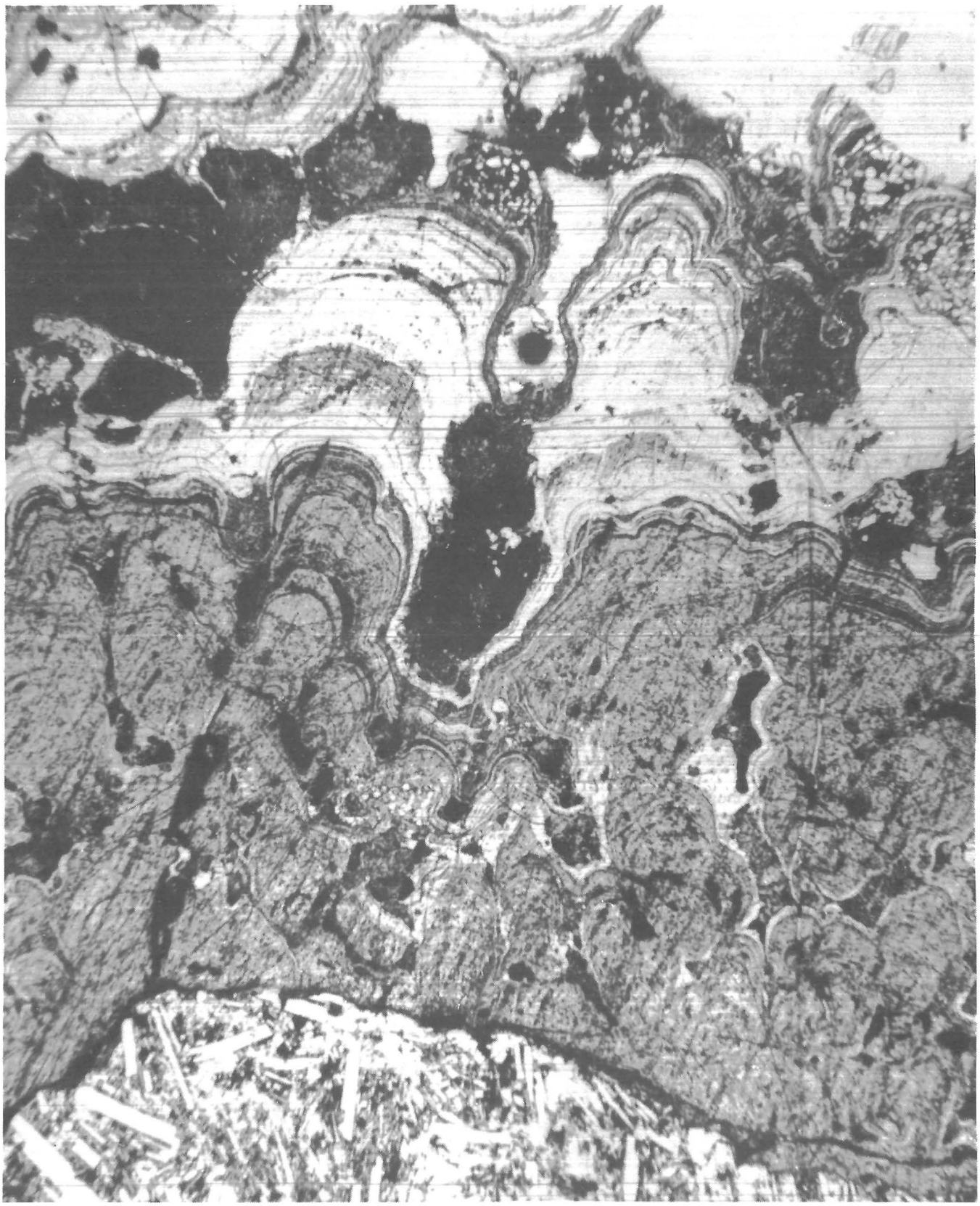

FIGURE A-7.—Sample O (X 32). Photomicrograph of polished section showing botryoidal manganese oxides at top, more iron-rich zones of manganese oxides in darker (tarnished appearance) middle zone, and trachytic sanidinite substrate at bottom, with lathe-shaped sanidine feldspar phenocrysts.

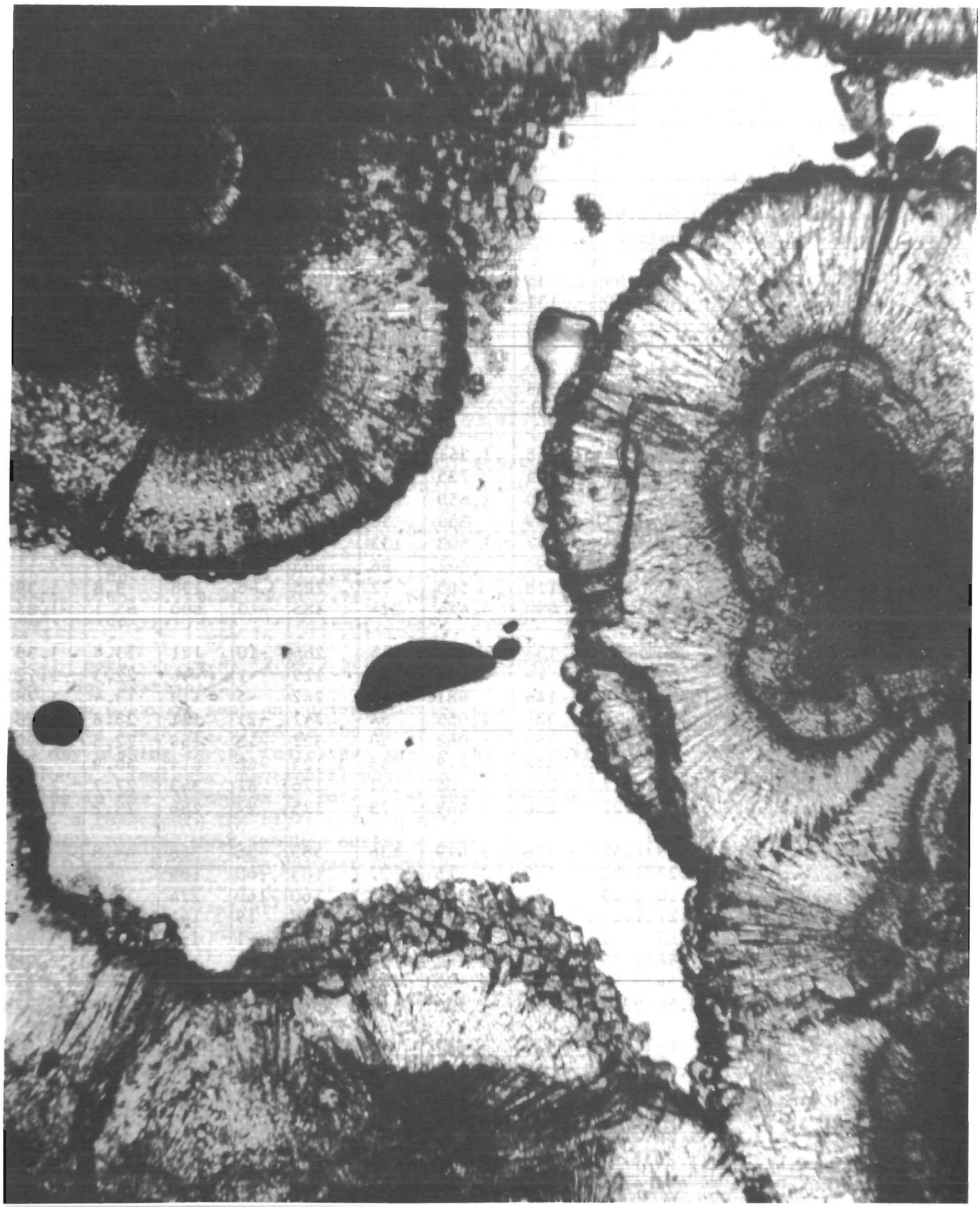

FIGURE A-8.—Sample D (X 32). Photomicrograph of thin section showing botryoidal phillipsite crystals encrusting altered basalt substrate.

APPENDIX B.--MECHANICAL CUTTING CHARACTERISTICS

TABLE B-1. - Results of crust and substrate drag bit test

Sample and test[1]	Crust and/or substrate	Spacing, cm	Depth of cut, cm		Force, N						Energy, J	Specific energy, J/cm^3
					Cutting		Normal		Side			
			Av	Max	Av	Peak[2]	Av	Peak[2]	Av	Peak[3]		
B:												
1a[4].	Crust....	NPT	0.50	0.95	186	645	86	231	4	59	3.7	[5]0.34
1b..	..do.....	NPT	.64	1.27	694	1,428	102	249	5	122	7.1	[5].66
C:												
1a..	..do.....	NPT	.39	.64	138	703	76	226	1	119	15.8	1.88
2a..	..do.....	2.54	.40	.70	131	601	68	251	-5	105	15.8	2.22
3a..	..do.....	2.54	.60	.81	95	672	49	294	-8	71	10.0	.91
1b..	..do.....	NPT	.64	.64	279	1,143	102	246	8	197	30.3	1.90
2b..	..do.....	2.54	.64	.64	220	1,090	91	276	-10	142	26.2	1.86
3b..	..do.....	2.54	.64	.64	306	1,081	58	216	-60	224	30.7	2.18
2c..	Both.....	NPT	.64	.64	138	569	30	181	1	137	11.6	.63
D:												
1a[4].	Crust....	NPT	.64	.64	245	1,361	81	480	-3	89	1.3	.32
1b..	..do.....	NPT	.62	.63	164	725	82	344	-12	213	13.7	1.55
2b[4].	..do.....	2.54	.89	.93	320	1,659	107	654	11	91	3.3	.26
3b[4].	..do.....	2.54	.96	1.17	79	355	50	100	3	21	1.3	1.17
1c..	Both.....	NPT	.64	.64	297	1,503	133	492	-32	201	21.5	[5]1.24
2c..	Both.....	2.54	.64	.64	190	1,241	98	435	-12	113	14.7	[5]2.11
3c..	Crust....	2.54	.64	.64	119	565	72	225	-6	138	9.8	1.39
2d..	Substrate	NPT	1.28	1.28	890	4,426	224	885	-13	600	65.1	[5]1.85
F:												
1a..	Crust....	NPT	.53	.91	133	578	65	266	-10	121	13.4	1.39
2a..	..do.....	3.18	.52	1.14	24	314	16	119	1	46	22.3	1.12
3a..	..do.....	3.18	.65	1.27	146	681	60	242	-5	119	13.4	1.28
1b..	..do.....	NPT	.57	1.27	331	1,059	84	247	-21	121	28.8	1.78
2b..	Both.....	3.18	.64	.64	159	1,068	50	322	-16	168	22.5	.90
3b[6].	..do.....	3.18	.64	.64	318	1,219	253	1,125	-60	614	40.9	.94
2c..	Substrate	NPT	1.27	1.27	395	1,708	33	176	87	343	27.7	1.35
2d[7].	..do.....	NPT	1.27	1.27	236	449	79	125	27	286	23.2	1.27
G:												
3a[8].	Crust....	NPT	1.19	1.57	476	1,619	136	583	-56	358	44.8	.48
4a[8].	..do.....	3.18	1.27	1.27	312	725	27	105	-60	189	8.2	.05
5b[6].	Substrate	NPT	2.10	2.29	196	364	95	160	-160	274	2.9	.03
4b..	..do.....	3.18	1.27	1.27	92	774	18	155	19	141	13.3	.58
3b..	..do.....	3.18	1.13	1.45	225	810	41	145	-1	138	31.9	.24
2b..	Crust....	3.18	1.46	1.78	197	1,361	67	525	3	122	14.7	.28
2c[6].	Substrate	NPT	2.54	2.54	1,040	2,122	242	405	-93	738	125.5	.61
4c[9].	..do.....	6.35	2.54	2.54	801	1,713	194	396	41	206	104.0	.77
H:												
2a..	Crust....	NPT	.93	1.68	307	1,281	92	349	13	199	36.0	.83
1a..	..do.....	3.81	.89	1.27	40	409	9	64	16	51	1.0	.01
3a..	..do.....	3.81	.83	1.27	432	1,325	131	408	11	307	31.3	1.11
1b[9].	Both.....	NPT	1.18	1.78	122	511	42	330	-22	108	13.2	.34
2b..	Substrate	3.81	1.36	2.22	111	463	25	176	-2	102	7.9	.16
3b..	..do.....	3.81	1.60	1.91	247	1,188	64	416	-105	556	27.8	.48

See explanatory notes at end of table.

TABLE B-1. -- Results of crust and substrate drag bit test--Continued

Sample and test[1]	Crust and/or substrate	Spacing, cm	Depth of cut, cm		Force, N						Energy, J	Specific energy, J/cm^3
					Cutting		Normal		Side			
			Av	Max	Av	Peak[2]	Av	Peak[2]	Av	Peak[3]		
I:												
2a[6].	Both.....	NPT	1.52	1.83	251	1,094	82	361	16	394	29.9	0.32
1b..	Crust....	NPT	.85	2.54	242	1,192	85	463	5	147	42.4	.85
2b..	Substrate	3.81	2.34	2.79	304	1,281	73	454	-76	434	56.0	.74
3b[6].	Both.....	3.81	2.17	2.49	395	1,192	94	219	-46	261	26.8	.10
2c..	Substrate	NPT	2.54	2.54	494	1,432	101	373	92	859	75.8	.60
J:												
2a[4].	Crust....	NPT	1.35	1.98	810	3,323	391	1,570	51	121	15.4	[5].30
2b..	..do.....	NPT	.93	1.27	373	1,690	141	636	33	151	27.7	.72
2c[10]	Both.....	NPT	1.27	1.27	1,619	4,213	876	1,632	-49	1,655	185.0	NA
M:												
1b[6].	Substrate	NPT	.32	.32	2,571	7,166	1,864	5,697	-52	480	48.9	4.86
2b..	..do.....	NPT	.32	.32	5,354	10,782	3,784	8,949	190	970	121.8	35.80
3b[6].	..do.....	NPT	.32	.32	7,460	13,425	5,822	10,613	-707	2,304	331.5	6.72
N:												
2a..	Crust....	3.81	.79	1.59	578	1,864	253	743	13	199	44.2	1.64
4a..	..do.....	3.81	.99	1.32	263	1,210	113	556	3	136	20.6	.86
Y:												
3a..	..do.....	NPT	1.88	2.54	663	4,146	278	1,810	23	327	128.0	.75
2a..	..do.....	3.81	1.30	1.63	322	2,411	129	934	-6	254	64.6	1.55
2b..	..do.....	NPT	1.91	1.91	1,441	4,319	520	1,708	-323	1,357	174.9	.78
3b..	..do.....	3.81	1.91	1.91	863	3,407	339	1,423	-15	361	132.5	.33
4b[4].	..do.....	3.81	1.19	1.32	275	1,130	104	430	-19	118	9.5	.04
2c[6].	..do.....	NPT	2.54	2.54	1,192	4,693	596	1,819	153	640	184.0	.14
3c..	Both.....	3.81	2.54	2.54	[5]6,303	[5]12,570	2,793	5,587	-82	1,392	[5]400.2	[5]1.00

NA Not available.

NPT No previous test on current cutting plane.

[1]Cutting tests performed in the order listed. B through Y refer to the sample number; any missing letter indicates sample was not suitable for cutting tests. Numbers 1 through 5 indicate horizontal position on sample; 1 starting at right side while looking in the direction of cut. Letters a through d refer to the vertical cutting plane, a represents the first cutting plane.

[2]Single highest peak reached during a test.

[3]Difference between the largest negative and positive side force.

[4]Sheared off sample's highest point.

[5]Best estimate considering crust-substrate mix or instrumentation problems.

[6]Broke to edge of sample.

[7]Kerf cutting only.

[8]Cuttings included large slabs of crust.

[9]Left significant core between current and previous test.

[10]Total sample destruction.

U.S. GOVERNMENT PRINTING OFFICE: 1987 - 605-017/60101 INT.-BU.OF MINES,PGH.,PA. 28570